A PERFORMANCE EVALUATION OF MILLIMETER-WAVE CELLULAR NETWORKS WITH USER MOBILITY

SHAMMA NABILA NIKHAT

A THESIS

IN

THE DEPARTMENT

OF

ELECTRICAL & COMPUTER ENGINEERING

PRESENTED IN PARTIAL FULFILLMENT OF THE REQUIREMENTS

FOR THE DEGREE OF THE MASTER OF APPLIED SCIENCE

CONCORDIA UNIVERSITY

MONTREAL, QUEBEC, CANADA

APRIL 2018

CONCORDIA UNIVERSITY
SCHOOL OF GRADUATE STUDIES

This is to certify that the thesis prepared

By: Shamma Nikhat

Entitled:

A PERFORMANCE EVALUATION OF MILLIMETER-WAVE CELLULAR NETWORKS WITH USER MOBILITY

and submitted in partial fulfillment of the requirements for the degree of

Master of Applied Science

Complies with the regulations of this University and meets the accepted standards with respect to originality and quality.

Signed by the final examining committee:

_____ Chair
Dr. R. Raut

_____ Examiner, External
Dr. C. Assi, CIISE To the Program

_____ Examiner
Dr. D. Qiu

_____ Supervisor
Dr. M. Mehmet-Ali

Approved by: _____
Dr. W. E. Lynch, Chair
Department of Electrical and Computer Engineering

_____ 20_____

_____
Dr. Amir Asif, Dean
Faculty of Engineering and Computer Science

ABSTRACT

A PERFORMANCE EVALUATION OF MILLIMETER-WAVE CELLULAR NETWORKS WITH USER MOBILITY

SHAMMA NABILA NIKHAT

Millimeter-Wave (mmWave) communications may be the key technology for the realization of 5G networks. MmWave communications have significantly different propagation characteristics than microwave (μWave) frequencies. The recent studies have determined the performance of cellular mmWave networks using stochastic geometry technique assuming a stationary user. The stationary user model doesn't capture correlation in the blocking of the links as the user moves on. In this work, we have determined the performance seen by a mobile user traveling over a path at constant and varying speeds. We have obtained the cumulative information received by the user as a function of its path length for different blocking intensities and cell sizes. The results show that while the received information rate doesn't vary significantly with mobility, the average path length that the mobile user is associated with a base station without interruption, drops down sharply with increasing blocking intensity. This will cause in high handover rate, which will result in high overhead. In this thesis, we have derived the probability distribution of path length that a user is associated with the same base station without interruption. This work demonstrates the significance of the user mobility on the performance of cellular mmWave networks.

.

ACKNOWLEDGEMENT

I would like to convey my deepest gratitude to my supervisor **Dr. Mustafa Mehmet Ali** for having faith in me and giving me this opportunity of this research work. Without his guidance and support this work would not be completed. His supervision gives me encouragement to move forward. I consider myself the luckiest, to have such a nice and considerate supervisor.

I would like to thank my parents, **Mr. Hafizur Rahman** and **Mrs. Meherun nessa** and my family for their love and guidance. Finally, I am always grateful to my husband **MD Tanveer Alamgir**, whose unconditional support and constant encouragement made this master's degree possible.

TABLE OF CONTENT

LIST OF FIGURES

LIST OF TABLES

LIST OF ACRONYMS

IOT	Internet of Things
EPC	Electronic Product Code
KPI	Key Performance Indices
5G	5th Generation Wireless Systems
MmWave	Millimeter Wave
4G	4th Generation Wireless Systems
µWave	Microwave
LTE	Long-Term Evolution
SIR	Signal-to-Interference Ratio
SINR	Signal-to-Interference-Plus-Noise Ratio
RAT	Radio Access Technology
3G	3rd Generation Wireless Systems
D2D	Device to Device
MIMO	Multiple-Input-Multiple-Output
LOS	Line-of-Sight
NLOS	Non-Line-of-Sight
PPP	Poisson Point Process
RWP	Random Waypoint Mobility Model
PMF	Probability Mass Function
Gbps	Giga Bits Per Second

LIST OF SYMBOLS

ρ	Densification Gain
λ	Base Station Intensity
Ψ	Set of Base Stations
b_ℓ	ℓ'th base station
(R_ℓ, φ_ℓ)	Polar Coordinates of The Station b_ℓ in The X-Y Plane
v_i	User Speed Over The i'th Interval
τ_i	Duration of The i'th Interval
$[a_i, b_i]$	Speed Range Over the Speed is Uniformly Distributed
β_i	Parameter of τ_i for exponential distribution
c	Proportionality Constant
P_T	Transmit Power
g_ℓ	Gamma Random Variable
N_ℓ	Gamma Distribution Parameter Value of a Link
M	Main Lobe Directivity Gain
m	Back Lobe Directivity Gain
θ	Beam Width of Main Lobe
G_i	Directivity Gain of the Link Between the Base Station b_i And the User
ϕ_U	Angle of Arrival of the Signal of the Link
ϕ_B	Angle of Departure of the Signal of the Link
G_0	Directivity Gain of the Tagged Base Station Link
$r_{\ell,y}$	Distance Between the Base Station b_ℓ and the User
$\alpha_{\ell,y}$	Exponent of the Power Loss

$p_{\ell,y}$	Floating Intercept of the Path Loss
σ_N^2	Additive Noise Power
B_W	User Bandwidth
N_F	Noise Figure in dB
$SINR_y$	Signal-to-Interference-Plus-Noise Ratio of the User When Its Distance from the Origin is y
K	Number of Blockings Over the Link $r_{k,y}$
Λ	Intensity of Blockings
L	Length of Blockings
T_{max}	Threshold Value of SINR
C_y	Information Receive Rate of the User at Location y
$P_C(T)$	SINR Coverage Probability of the User
$P_R(\mu)$	Rate Coverage Probability
μ	Rate Threshold Value
A	Rectangular Region with an Area
M	Number of Independent Runs
Δy	Segment Size
r	Average Cell Radius
$\|XY\|$	the points X and Y and the length line segment
F_ℓ	Probability of No Handover is at Least ℓ Steps
P_ℓ	Probability of No Handover is ℓ Steps

CHAPTER 1

INTRODUCTION

1.1 INTRODUCTION

Internet of Things (IoT) is a new paradigm that is expected to change our way of life. 5th generation (5G) wireless networks under consideration is the key enabling technology for IoT. Millimeter wave (MmWave) networks is one of the proposed solutions for 5G and the objective of this thesis is the performance evaluation of mmWave networks.

1.2 INTERNET OF THINGS (IOT)

The European Research Cluster defines Internet of Things (IoT) as, “A dynamic global network infrastructure with self-configuring capabilities based on standard and interoperable communication protocols where physical and virtual “things” have identities, physical attributes, and virtual personalities and use intelligent interfaces, and are seamlessly integrated into the information network" [22].

It is expected that by the year 2020 about 50 billion devices will be connected through internet [15]. The “thing” is defined in [23] as, “A thing is any object with embedded electronics that can transfer data over a network-without any human interaction”. Several household domestic appliances i.e. fridge, lights, temperature and home security is now also connected through internet [16]. There are also many devices such as automobile components, wearable devices, factory machines and also environmental sensors are now included to the IoT [23].

In [17], the vision of Internet of Things are characterized into three main parts; object, connectivity and semantics. In the object vision, we can track any device through sensors and it can be identified by the Electronic Product Code (EPC) [17]. The second vision is to connect these sensor based objects through internet [17]. The third one that is semantic oriented vision states the communication between different objects is through internet [16].

1.3 GOALS OF INTERNET OF THINGS

Integration of sensors and sensor based systems were the new introduction to the internet of things platform [18]. Further innovation in IoT are cloud computing and fog paradigm [18]. Internet of services is the new platform in service era. All the electronic and electronically stimulated products will be considered for Internet of Things involvement. It is expected that by 2025 people will not buy the products but will subscribe to the services provided by these products [25]. In the near future the mobile devices and all other domestic or industrial devices will be connected through internet [16]. In [21] the devices of IoT have been divided into six categories i.e. smart homes, smart business, smart cities, security, surveillance and healthcare. High-speed internet and huge bandwidth are needed to provide user access to these products connect anytime anywhere [16].

1.4 INTERNET OF THINGS (IOT) AND 5G

In the near future, the demand for wireless communications will continue to grow as the volume of data, the number of devices and the data rates will keep up rising rapidly [1]. The 5G networks is to be designed to meet the future communication demands of the users. High scalability, high capacity, energy saving, reduced latency, quality of service, heterogeneity, efficient network and spectrum, built-in redundancy, security and privacy, all these features are needed in the 5G technologies to provide expected services of IoT [16]. 5G can support IoT by providing communication between devices, achieving high data rates, saving energy and reducing latency [16].

1.5 REQUIREMENTS OF 5G

Samsung has provided 7 Key Performance Indices (KPI) as the requirements of 5G [24]. But not all the requirements need to be met up simultaneously because the performance of different applications has different requirements [1]. These performance indices are described below,

1. **Peak Data Rate:** In any network the best rate that the user can achieve. It is required that the low-mobility user in 5G systems can achieve data rates of 10-50 Gbps [19].
2. **Cell Edge Data Rate:** In general, at the edge of the cell the user can receive less data but in 5G this problem is overcome by achieving the same rate in any location of the user [19].
3. **Latency:** 5G will provide lower latency than 4G, it needs to achieve about 1ms roundtrip latency [1].
4. **Cell Spectral Efficiency:** The most important feature of 5G is that it should provide coverage of network in a wide area and should handle heavy traffic flow. 1000 fold capacity per km^2 should be achieved than Long-Term Evolution (LTE) [19].
5. **Mobility:** Users with different velocities should achieve higher data rate in 5G systems. To optimize with mobility high speed should be supported by small cells. With small cells the position of a device can also be measured accurately [19].
6. **Instantaneous Connection:** To support cloud computing and IoT, 5G needs to support simultaneous connection for large number of different devices [19].
7. **Cost Efficiency:** Cost is always an important parameter for establishment of a technology. 5G needs to increase its capacity with reduced price to be a good future network [19].

1.6 PROPOSED SOLUTIONS TO 5G

Among all the requirements of 5G the most essential one is achieving high data rate than LTE. Three solutions have been proposed to 5G [1],

- Millimeter Wave spectrum
- Small cells
- Massive MIMO

Next we will discuss these solutions,

1. **Millimeter Wave Spectrum:** The 5G needs to increase the network capacity by an order of magnitude compared to 4G networks in order to meet the increasing demands [2]. This will require substantial amount of new spectrum. Most of the spectrum at the microwave (μWave) frequencies (<6 GHz), is already heavily utilized and only mmWave frequencies (30 GHz – 300 GHz) has large amount of unutilized spectrum available. Until now, mmWave spectrum is considered to provide poor communications environment due to its hostile propagation characteristics, such as strong path loss, atmospheric absorption, high penetration losses and low diffraction. As a result, mmWaves are susceptible to severe blocking effects [1-3]. However, the advances in technology are overcoming these obstacles [1]. Next we will discuss these propagation characteristics,

    - Path loss: when the frequency is raised the free space-path loss between the antennas increases with the carrier frequency [1]. The higher frequencies can experience high path loss than the lower frequencies. By using multiple

antennas in limited space, the transceivers can provide array gain that minimizes the frequency dependent path loss [7].

- Atmospheric and Rain absorption: mmWave communication is also affected by rain attenuation, atmospheric and molecular absorption characteristics, but by minimizing the size of the cells (approximately 200m) this effect can be reduced [20].

- Blocking: mmWave is very sensitive to blockages. The link between BS and user should be line-of-site to built proper connectivity. New channel models using directional antennas, system-level analysis and simulation studies are now done to overcome the effect of blocking [1].

- Highly Directional: beams of mmWave is significantly directional, it changes the behavior of the interference entirely [1]. The beam training procedure and different algorithms are needed to direct the transmit and receive beams [20].

2. **Small Cells:** small cells can effectively raise the capacity of the network [1]. Different types of cell sizes can perform different capacity and coverages of the network such as, femtocells, picocells and microcells [16]. By lowering the cell sizes, spectrum reuse can be done in a specific area. But at the same time, signal-to-interference ratio (SIR) is increased in a dense network [1]. Below we discuss some of the challenges faced by small cell networks:

    - BS densification gain ($\rho > 0$) is a ratio of increase of data rate of the network to increase of the density of base stations in the network. When the network densifies the signal-to-interference-plus-noise ratio (SINR) increases because

signal power increases in noise-limited network, and lightly loaded small cells produce lower interference in interference-limited network [1].

- In mmWave networks, the network is noise- limited in the high frequency and when the network densifies it lowers the load and also it separates cell resources that's why high gain can be achieved $\rho \gg 1$ [1].

- As the networks now are becoming heterogeneous so the multi-RAT (Radio Access Technology) network need to connect user with different types of frequency bands, also for other technologies such as 3rd Generation (3G), LTE, Device to Device (D2D) [1]. In a multi-RAT network great challenge is to maintain the load balancing of BSs, utilization of radio recourses etc. "Biasing" and "blanking" are the two procedures to manage the network. Biasing is connecting the user with a small cell instead of a macrocell and also handing over the user to a small cell when the macrocell is loaded heavily. Blanking is shutting down the transmission of macrocell when the small cell is serving the biased users. In mmWave networks the interference is low that's why it reduces the need of blanking [1].

- Modeling and analysis of mobility in a network is always difficult. The dense and heterogeneous networks introduce different challenges in the performance of a mobile user. In mmWave networks the transmit and receive beams has to be aligned that's why the handovers are difficult [1].

- Cost is an important issue for the deployment of small cells. Permission for a site, using reliable backhaul connections, rent of the site are the reasons for

higher cost for the small cell networks [1].

3. **Massive MIMO:** the idea of **"**massive MIMO" was initially called as "large–scale antenna systems". In the system the base stations were equipped with large number of antennas compared to the active users using each time-frequency signaling resources. The number of antennas per base station will be in hundreds if the user per resource is in tens [1]. Below some challenges of massive MIMO systems has been explained:

    - To provide clear channel estimates, pilot transmission has to be orthogonal among users of the same cell and should be reused, otherwise all the resources will be occupied by pilots. The interference called "pilot contamination" remains same even with the large number of antennas in BS.
    - There are architectural complexities for the vision of massive MIMO system. High-power amplifiers are needed to feed sector antennas, low-power amplifiers are needed for tiny antennas, scalability, antenna correlations and mutual couplings, cost etc are issues of massive MIMO architecture [1].
    - Channel models need wide-ranging field measurements. Antenna correlations and couplings should be evaluated for vast antenna arrays, actual channel orthogonalization should be verified, the impact of the channel model should be evaluated [1].
    - The need for massive MIMO system will vanish if the network become dense with small cells as the number of active users per cell will decrease.

Among the proposed solutions for 5G, this thesis considers mmWave networks being essential in meeting requirements of 5G.

1.7 RELATED WORK

The growing interest in mmWave communications for 5G networks have led to various measurement studies to determine its channel propagation characteristics [4, 5]. The measurements have shown that propagation of line-of-sight (LOS) and non-line-of-sight (NLOS) mmWave signals in free space significantly differ from each other. Following these measurements, there have been several system modeling studies of cellular mmWave networks.

Recently, stochastic geometry has emerged as a technique for modeling μWave cellular networks [6]. Stochastic geometry assumes that the base stations are distributed according to a homogeneous Poisson Point Process (PPP) in the Cartesian plane as opposed to placing them on a grid. This technique is mathematically more tractable compared to grid modeling and it provides as much accurate results.

In [3, 7-10], the stochastic geometric modeling has been extended to the mmWave cellular networks. In [3], they assume that the blockages are also distributed according to another PPP process. A link will be in the LOS state if it doesn't experience any blockings and otherwise it will be in the NLOS state. They assumed that user link to each of the base stations may experience blockages according to an independent Bernoulli trial. The user is associated with the base station with the highest receive power. In [7], they derive downlink SINR and coverage probability and information receive rate that takes into account LOS/NLOS status of the links for a user located at the origin. For LOS and NLOS base stations two different path loss exponent has been applied and their locations have been represented by two independent non-homogeneous PPP. For dense networks the location of the user in LOS region is approximated by a fixed LOS ball. Results show that dense mmWave network get higher

achievable rate than conventional networks because of large available bandwidth. In [8], stochastic geometry baseline analytical approach has been presented to compute statistical distribution of downlink SINR and data rate considering two main challenges of mmWave i.e. blocking effects and high directionality. The mmWave system is more likely to be noise-limited because of higher carrier frequency. If the network is dense then blockages also increased and it increases the noise and also it blocks the interfering signals, so the noise become more dominant than the interference. But there is an optimal density of base station after which the performance of the network drops. In [9], it is shown that considering the base station density, the noise-limited approximation is quite accurate. It is observed numerically that if the cell radius is equal to or higher than 100 meters then the mmWave cellular network can be considered to be noise-limited. For the state of the link to be LOS, two ball approximation is also introduced. In [10], the self-backhauling among BSs has been integrated to the conventional macrocellular networks to characterize the rate distribution in mmWave cellular networks. It shows that bandwidth has minimum impact on power and noise-limited cell edge users and base station density actually improves the rate. However, these results apply to a stationary user and donot give us insight into the performance that may be seen by a mobile user.

Mobility modelling is a necessary first step to explore the role of mobility in cellular networks, particularly handover rate [14]. The expected number of handovers per unit time is defined as handover rate [14]. Handover rate is usually dependent on the cell radius, speed of the user and blockage intensity of the network. The rate is low for large cells and/or low mobility [14]. Handover is also dependent on the LOS and NLOS links for mmWave networks.

For the case of handoff, several works have been done for the mobile user, but those are limited to microwave cellular networks. In [14] they obtained the handoff rate for tractable random waypoint mobility model (RWP) and compared it to the classical RWP model. They have also compared the mobility results for hexagonal and Poisson-Voronoi tessellation, the two different models of cellular networks. Another stochastic geometry analysis framework has been proposed in [13] of mobile user to evaluate the handoff rates for different types of handoffs i.e. horizontal and vertical handoffs. In this work we are focusing on the mmWave cellular networks and try to evaluate handover characteristics for mobile user.

1.8 ORGANIZATION AND CONTRIBUTION OF THE THESIS

The objective of our work is to determine the performance seen by a mobile user in a mmWave cellular network. As the user moves along a path, the status of the links to the base stations will change but the blocking of the links may be correlated. We assume that the user will move along a straight path with either constant or variable speed.

The remainder of the thesis is organized into following chapters,

- In chapter 2, as the system model appears to be mathematically not tractable, we have evaluated performance of this system through Monte Carlo simulation. We have determined the total amount of information received by the user as a function of its path length for different cell sizes and blocking intensities. The results show that the average path length that the user is associated continuously with the same base station depends on blocking intensity. The average path length drops sharply as blocking intensities rise.

- In chapter 3, we have studied uninterrupted path length of the mobile user. We have derived analytically probability distribution of the path length that the user

remains associated with the same tagged base station. We also evaluate that the probability of handover is dependent on the path length covered by the mobile user.

- In chapter 4, conclusion of the thesis and future work is presented.

CHAPTER 2

THE PERFORMANCE EVALUATION OF MMWAVE CELLULAR NETWORKS WITH USER MOBILITY

2.1. INTRODUCTION

The propagation environment is one of the distinguishing features of the mmWave cellular communication [7]. As mmWave signals are interrupted by certain materials like concrete walls cause severe penetration loss, so it is more sensitive to the blockages of the network than microwave frequency bands [7]. Blockages cause substantial differences in the line-of-sight (LOS) paths and non-line-of-site (NLOS) path loss characteristics [7]. Research shows that there are three main reasons for which mmWave is sensitive to blockages; first high penetration losses when passing through many common materials, second mmWave frequencies donot diffract well in terrestrial environments and third because of the requirement of directionality.

In this chapter we have determined performance seen by a mobile user in a mmWave cellular network with different blocking intensities. We evaluated different parameters of the network and observed the effects when the blocking intensity and cell radius are changed.

2.2. SYSTEM MODEL

We will consider a cellular network where base stations are located according to a Poisson Point Process (PPP) with intensity λ in the Cartesian plane. We will assume that the user travels along the positive y-axis starting from the origin. The system has three components, which are the base stations, the user and the links between the user and the base stations. Next, we describe each of these components,

i) Base Stations: We let $\Psi = \{b_\ell\}$ denote the set of the base stations where b_ℓ represents the ℓ'th base station and let (R_ℓ, φ_ℓ) denote the polar coordinates of the station b_ℓ in the

x-y plane. Since the intensity of the base stations is given by λ, average cell size is given by $1/\lambda$.

ii) The mobile user: The user will travel along the positive y-axis starting from the origin with either constant or variable speed. In the case of variable speed, the user speed will change after random time intervals. We let v_i and τ_i denote the user speed over the i'th interval and duration of the i'th interval respectively. We assume that v_i is uniformly distributed over the speed range $[a_i, b_i]$ and τ_i is exponentially distributed with parameter β_i respectively. Thus the probability density functions (pdfs) of v_i and τ_i are given by,

$$f(v_i) = \frac{1}{(b_i - a_i)}, a_i < v_i < b_i, \quad f(\tau_i) = \beta_i e^{-\beta_i \tau_i}, \tau_i \geq 0 \tag{2.1}$$

The mean values of v_i and τ_i are given by,

$$\bar{v}_i = \frac{1}{2}(a_i + b_i), \qquad \overline{\tau_i} = \frac{1}{\beta_i} \tag{2.2}$$

We will assume that the absolute value of the difference between the user speed and mean user speed over an interval is inversely proportional to the mean duration of the corresponding interval,

$$\bar{\tau}_i = \frac{c}{|v_i - \bar{v}_i|} \tag{2.3}$$

where c is the proportionality constant. As a result, the mean user speed decreases with the increasing mean duration of the random interval. Thus the user will spend less time in higher and lower speeds, which is reasonable.

Its possible to use other distribution for user speed than uniform distribution, such as truncated Gaussian distribution.

iii) The links between the user and the base stations: the user will be associated at any time with the base station that the user has the highest receive power. We will refer to this base

station as the tagged based station and let b_0 denote the tagged base station. We assume that the transmit power is a constant given by P_T and standard power loss model applies with α. The value of α will depend on whether the link between the user and a base station is LOS or NLOS. We assume that each link may experience independent Nakagami fading with different parameter values for LOS and NLOS links. As a result of fading, the received power at the user will be attenuated according to a normalized gamma distribution. We let g_ℓ denote the gamma random variable for the link of base station b_ℓ and N_ℓ the gamma distribution parameter value of this link. We assumed that the Nakagami fading parameter value will have the values of N_ℓ =3 and 2 for LOS and NLOS links respectively [7].

Next we will determine signal-to-interference-plus-noise ratio (SINR) of the down links as the user travels along the y-axis. We will assume that directional beamforming is being implemented which is approximated by a sector antenna pattern as in [7]. From [7], the parameters of the sectored antenna are given in the Table 2.1., where M, m denote main lobe and back lobe directivity gain respectively and θ the beam width of the main lobe. The subscripts B and U refer to a base station and to the user respectively. We let G_i denote the directivity gain of the link between the base station b_i and the user and ϕ_U and ϕ_B the angle of arrival and departure of the signal on this link. If the link is to the tagged base station, then $\phi_U = \phi_B = 0$, on the other hand for an interfering link they will be uniformly distributed over the interval $[0,2\pi]$. The directivity gain of the tagged base station link will be $G_0 = M_B M_U$ and for the interfering link i will be $G_i = a_k$ for $i > 0$ with probability p_k, $k = 1,2,3,4$, where a_k, p_k are defined in Table 2.1. with $c_B = \frac{\theta_B}{2\pi}$ and $c_U = \frac{\theta_U}{2\pi}$.

k	1	2	3	4
a_k	$M_B M_U$	$m_B M_U$	$M_B m_U$	$m_B m_U$
p_k	$c_B c_U$	$(1-c_B)c_U$	$c_B(1-c_U)$	$(1-c_B)(1-c_U)$

Table 2.1. Probability mass function of directivity gain G_i.

We let $r_{\ell,y}$ denote the distance between the base station b_ℓ and the user when the user's distance from the origin is y, and $\alpha_{\ell,y}$ denote the exponent of the power loss and $p_{\ell,y}$ floating intercept of the path loss formula of the corresponding link [3, 5, 9]. $\alpha_{\ell,y}$ and $p_{\ell,y}$ have different values for LOS and NLOS links and $p_{\ell,y}$ also depends on the carrier frequency of the system. Then the received signal power from this base station will be $g_\ell P_T G_\ell p_{\ell,y}\, r_{\ell,y}^{-\alpha_{\ell,y}}$. There will be constant additive noise power with value of σ_N^2. The noise will be dependent on the user bandwidth (B_W) and will be given by [9-10],

$$\sigma_N^2(dBm) = -174 + 10log_{10}B_W + N_F \tag{2.4}$$

where $N_F$is the noise figure in dB.

Let $SINR_y$ denote the signal-to-interference-plus-noise ratio of the user when its distance from the origin is y,

$$SINR_y = \frac{g_0 P_T G_0\, p_{0,y} r_{0,y}^{-\alpha_{0,y}}}{\sigma_N^2 + \sum_{b_i \epsilon (\phi/b_0)} g_i P_T G_i p_{\ell,y}\, r_{i,y}^{-\alpha_{i,y}}} \tag{2.5}$$

where the summation in the denominator denotes interference seen by the user from the other stations and $\alpha_{k,y}$ is defined as,

$$\alpha_{k,y} = \begin{cases} 2 & \text{if link } r_{k,y} \text{ is } LOS \\ 4 & \text{if link } r_{k,y} \text{ is } NLOS \end{cases} \tag{2.6}$$

Next, we present the probability mass function (pmf) of the random variable $\alpha_{k,y}$. Let K denote the number of blockings over the link $r_{k,y}$ and Λ the intensity of blockings.

Modeling the blockings as line segments with length L, in [3], it has been shown that K has a Poisson distribution with mean $\gamma r_{k,y}$ where $\gamma = \frac{2\Lambda}{\pi} E[L]$. Thus if a link doesnot have any blockings then it is LOS otherwise it is NLOS. From the Poisson distribution, we determine the pmf of $\alpha_{k,y}$,

$$Prob(\alpha_{k,y} = 2) = Prob(K = 0) = e^{-\gamma r_{k,y}} \tag{2.7}$$

$$Prob(\alpha_{k,y} = 4) = Prob(K > 0) = 1 - e^{-\gamma r_{k,y}} \tag{2.8}$$

Assuming that the user achieves Shannon bound for instantaneous SINR, then the information receive rate of the user at location y is given by [7],

$$C_y = B_W \ln(1 + \min(SINR_y, T_{max})) \tag{2.9}$$

In the above, T_{max} is a threshold and $\min(SINR_y, T_{max})$ is used as very high SINRs may not be exploited due to limiting factors like linearity in the radio frequency front end [7]. The received information rate of the user is a variable since as the user travels along the y-axis its distances to the base stations change.

Next we define performance measures used in the simulation. The SINR coverage probability of the user is defined as,

$$P_C(T) = Prob(SINR > T) \tag{2.10}$$

which is the probability that the SINR seen by the user will be greater than a target value T during the path of its travel.

Rate coverage probability is defined as,

$$P_R(\mu) = Prob[C_y > \mu] \tag{2.11}$$

which is the probability that the achievable rate seen by the user will be greater than some threshold value μ during the path of its travel.

2.3. SIMULATION ENVIRONMENT

We have determined the performance of mmWave communications with user mobility through Monte Carlo simulation. We have performed M independent runs and took average of the results. In the simulation the user moves in small segments of length Δy along the y-axis. It has been assumed that during each segment the user will continue to receive information at the constant rate corresponding to the rate at the beginning of the segment. Next, we describe the main components of the simulation,

2.3.1. BASE SATIONS

The base stations are generated according to a Poisson process with the intensity of λ stations/m^2 and the cellular network will be assumed to cover a rectangular region with an area of $A = XY$ where X and Y are the width and length of the rectangle. The rectangle is placed such that its length is parallel to the y-axis and the user path is completely within the rectangle. In each run, we determine the number of base stations within the cellular network by generating a Poisson random value with the parameter λA. Then, we determine x and y coordinates of each base station by generating uniformly distributed random numbers in the intervals $(-\frac{X}{2}, \frac{X}{2})$ and $(-\frac{Y}{2}, \frac{Y}{2})$ respectively.

2.3.2. BLOCKINGS

Following [3], the number of blockings has been generated according to a Poisson process with the intensity of Λ blockings/m^2. For simplicity, it's assumed that the blockings consist of lines and the center of each blocking is uniformly chosen in the cellular network area. Then, the angle of each blocking line is uniformly chosen in the interval $(0, 2\pi)$.

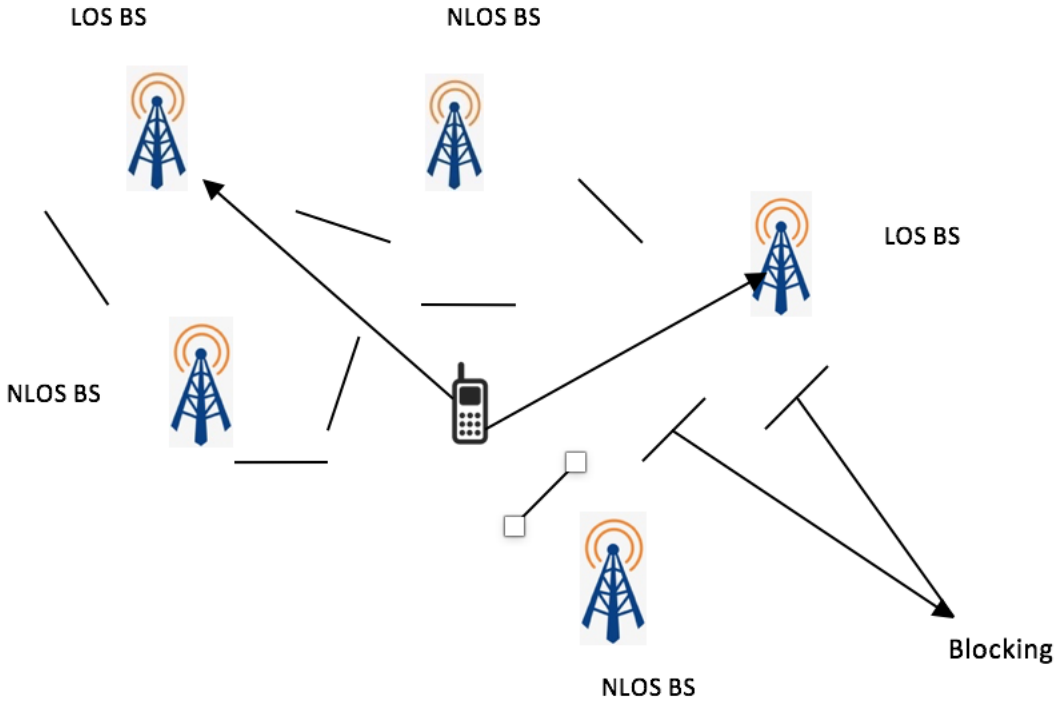

Fig. 2.1. System model with blockages for mmWave cellular networks

2.3.3. USER MOBILITY

In simulation, we have assumed that the user moves in segments of length Δy along the y-axis. At each position, the status of the link between the user and each base station is determined by finding out if the link intercepts any of the blockings as shown in Fig. 2.1. If the link doesn't intercept any blockings, then it's LOS and otherwise it's NLOS.

2.4. SIMULATION RESULTS

In this section we present the simulation results. The results have been obtained by performing M=10 independent runs and then taking their average. We have set the

segment size to $\Delta y = 1m$. We assumed that the carrier frequency of the system is 28GHz and the user bandwidth is $B_W = 2\ GHz$. From Table 2.1. in [5], floating intercepts of the path loss formula are 61.4dB and 72dB for *LOS* and *NLOS* links respectively. As a result, $p_{\ell,y}$ is set to $10^{-6.14}$ and $10^{-7.2}$ for *LOS* and *NLOS* links respectively. Transmit power is set to $P_T = 1W$, and the values of antenna parameters are $M_B = M_U = 10\ dB$, $m_B = m_U = -10dB$ and $\theta_B = 30^0$, $\theta_U = 30^0$. The receiver noise figure is assumed to be $N_F = 10dB$, the average length of line blockings has been set to $\bar{L} = 30m$ and $T_{max} = 20dB$. The results have been plotted for different average cell radiuses and blocking intensities. The average cell radius (r) is determined as the radius of a circle that has the average cell size through the relation, $\lambda = \frac{1}{\pi r^2}$. Initially, we have assumed a constant user speed of 1m/s. The simulation results have been generated by the Matlab program that is the the Appendix A.1.

In Fig. 2.2 we plot the average information rates (Gbps) as a function of the user distance from the origin with blocking intensity 10^{-3} for average cell radius of 50m. In this figure it is seen that the information rate fluctuates as the user moves. As the cell radius is small and the blockage intensity is high the user has more handovers and thus the rate fluctuates. When the user moves a small segment Δy, tagged base station may change because at each point it is determining which base station is LOS and try to connect with that base station. If all the base stations become NLOS then it will connect to the base station with smallest distance. In Fig. 2.2, it can be also observed that at the distance of approximately 100m and 200m, sudden spikes on the information rate. This types of spikes appears when all the interfering base stations become NLOS and only the tagged base station is LOS. In this case, the interference becomes very low and thus information rate becomes very high.

Fig. 2.3 shows state of the tagged base station as LOS and NLOS, LOS is indicated by '1' and NLOS is indicated by '2'. As may be seen, in this case tagged base station is almost always LOS except for few instances.

Fig.s 2.4-2.6 plot the total amount of received information as a function of the user distance from the origin with blocking intensity as a parameter for cell radiuses of r =50m, 100m and 200m respectively. As may be seen, in each cell radius the amount of received information is increasing almost linearly with waves and different slopes determined by blocking intensity. We also note that the total amount of received information drops with increasing cell size.

Table 2.2 presents the average information receive rate, which is determined by dividing the total amount of received information by the end of the path with the user travel time. Table 2.3. presents the received information rate of a stationary user at the origin for the same cell sizes and blocking intensities. From Table 2.2-2.3, average information receive rate drops down with increasing cell sizes and blocking intensity. We note that, the average information rate of the mobile and stationary user is similar.

Table 2.4. and 2.5. represent the probability that a tagged base station is NLOS and the probability that a link is NLOS respectively for different cell radiuses and blockage intensities. It can be observed that when there is no blockage or the blockage intensity is very low, the probability of a tagged base station is being NLOS is zero. This probability increased when the blockage intensity is higher. In Table 2.5. the probability of links being NLOS increases with the increasing blockage intensity.

Table 2.6. presents the average path length for uninterrupted user association to a tagged base station for different cell radiuses with blockage intensity as a parameter. It may be

seen that the average path length sharply drops down with increasing blockage density at any cell size. Fig.s 2.7, 2.8 and 2.9 present number of observations for uninterrupted path length for cell radius of 100m for no blocking and blocking intensities of 10^{-4} and 10^{-3} respectively. It may be seen that even light blocking results in many short path lengths. Thus high blocking intensities will result in very high handover rates.

Next, we present results for variable user speed. Fig. 2.10. shows the total amount of received information as a function of user distance from the origin for cell radius of 100m with blocking intensity as a parameter for uniformly distributed speed in the range of [1m/s,6m/s] for mean random interval duration of 30s. The total amount of received information has also dropped down as the user covers the path in shorter time.

Next, in Fig.s 2.11 and 2.12 we present rate coverage probability and SINR coverage probability for both stationary and mobile users with constant speed of $1\,ms^{-1}$ respectively. We assumed that the user bandwidth is $\mathrm{B_W} = 2\ \mathrm{GHz}$, blockage intensity is $\Lambda = 0.001$ and cell radius is $r = 50m$. From the figures it can be observed that both the SINR coverage probability and achievable rate probabilities for mobile user are very similar to that of a stationary user.

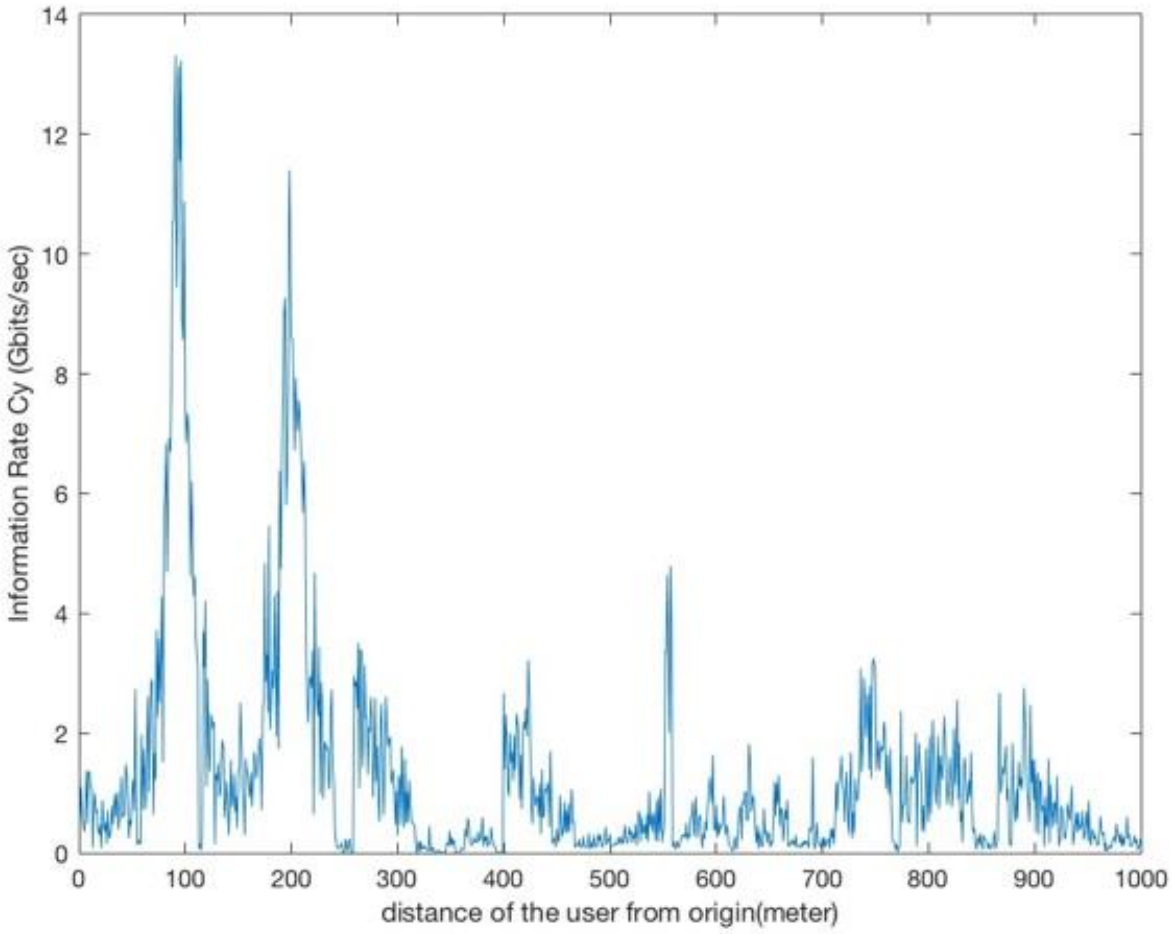

Fig. 2.2. Average information rate (Gbps) vs distance of the user from the origin for cell radius of 50 m ,blocking intensity of 10^{-3} and user speed of 1m/s.

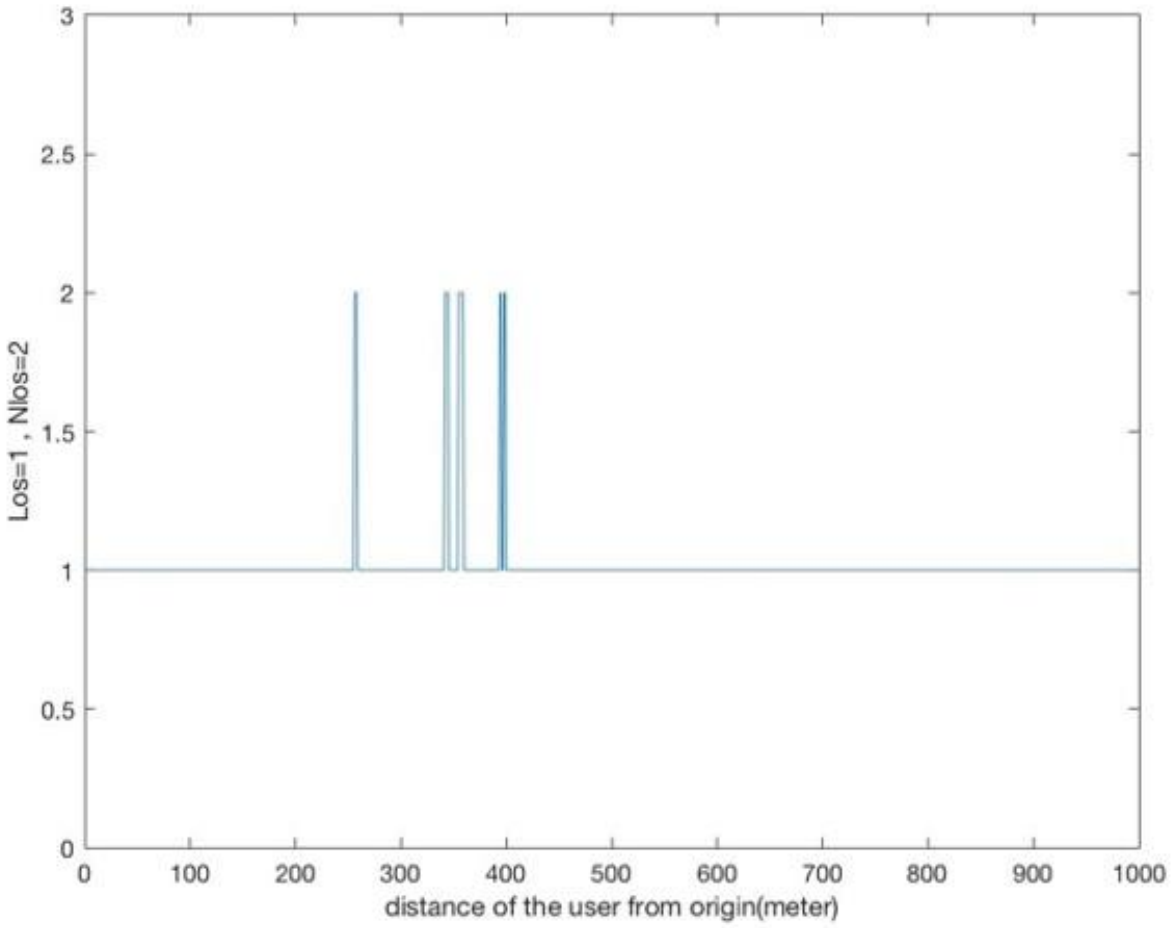

Fig. 2.3. The tagged base station is LOS or NLOS vs distance of the user from the origin for cell radius of 50 m ,blocking intensity of 10^{-3} and user speed of 1m/s.

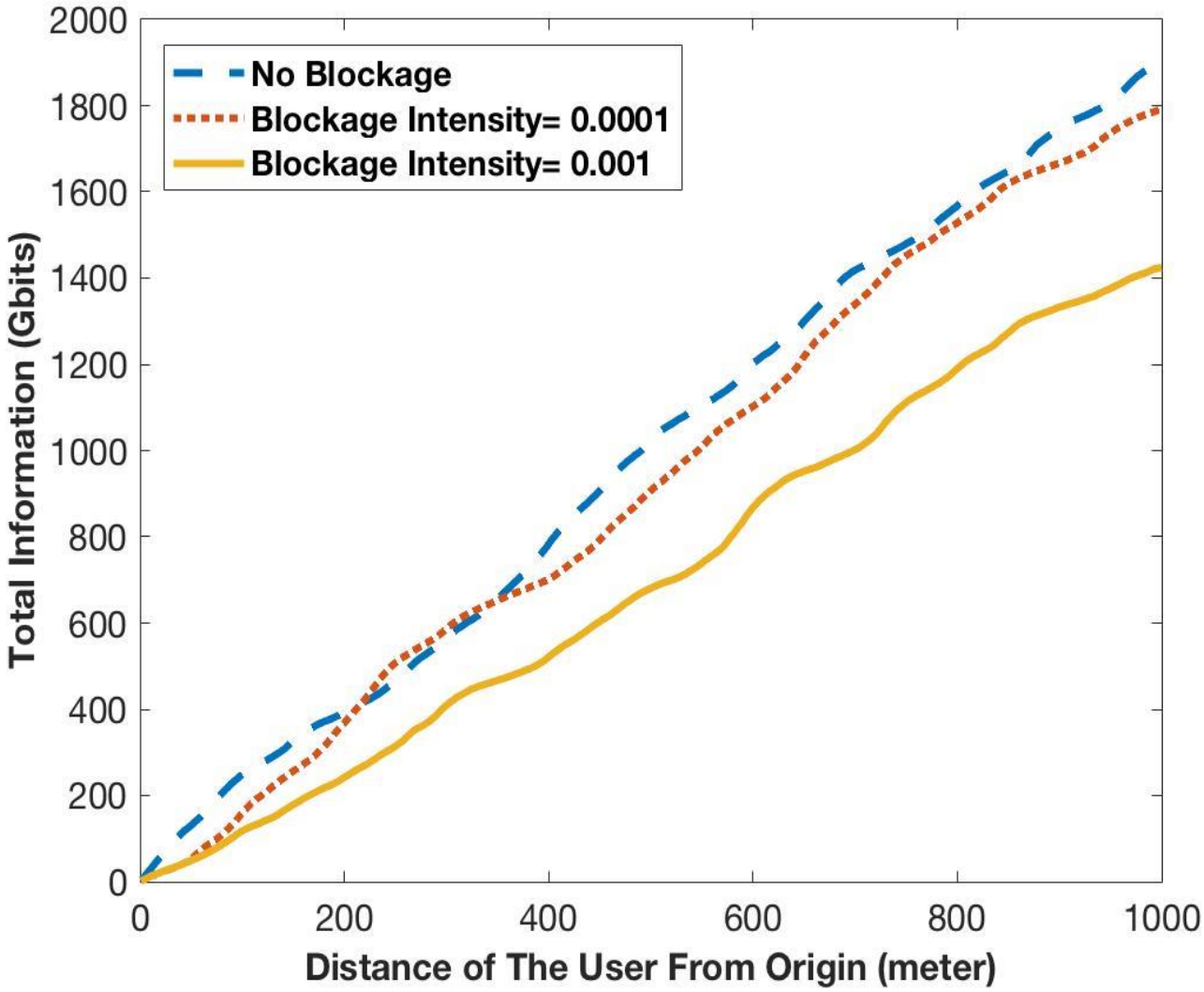

Fig. 2.4. Total information received (Gbits) vs distance (meter) of the user from the origin for cell radius of 50 m for user speed of 1m/s.

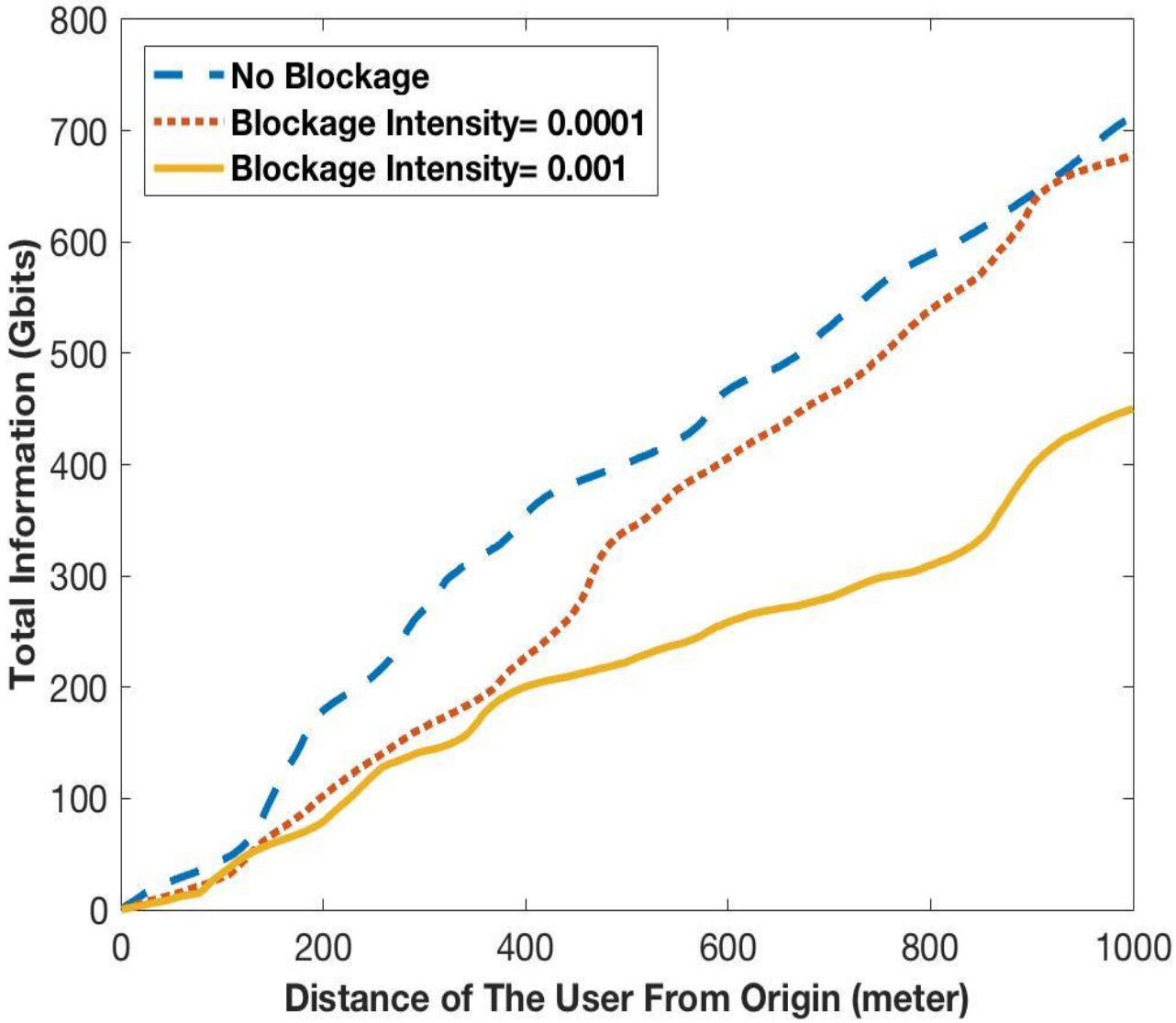

Fig. 2.5. Total information received (Gbits) vs distance (meter) of the user from the origin for cell radius of 100 m for user speed of 1m/s.

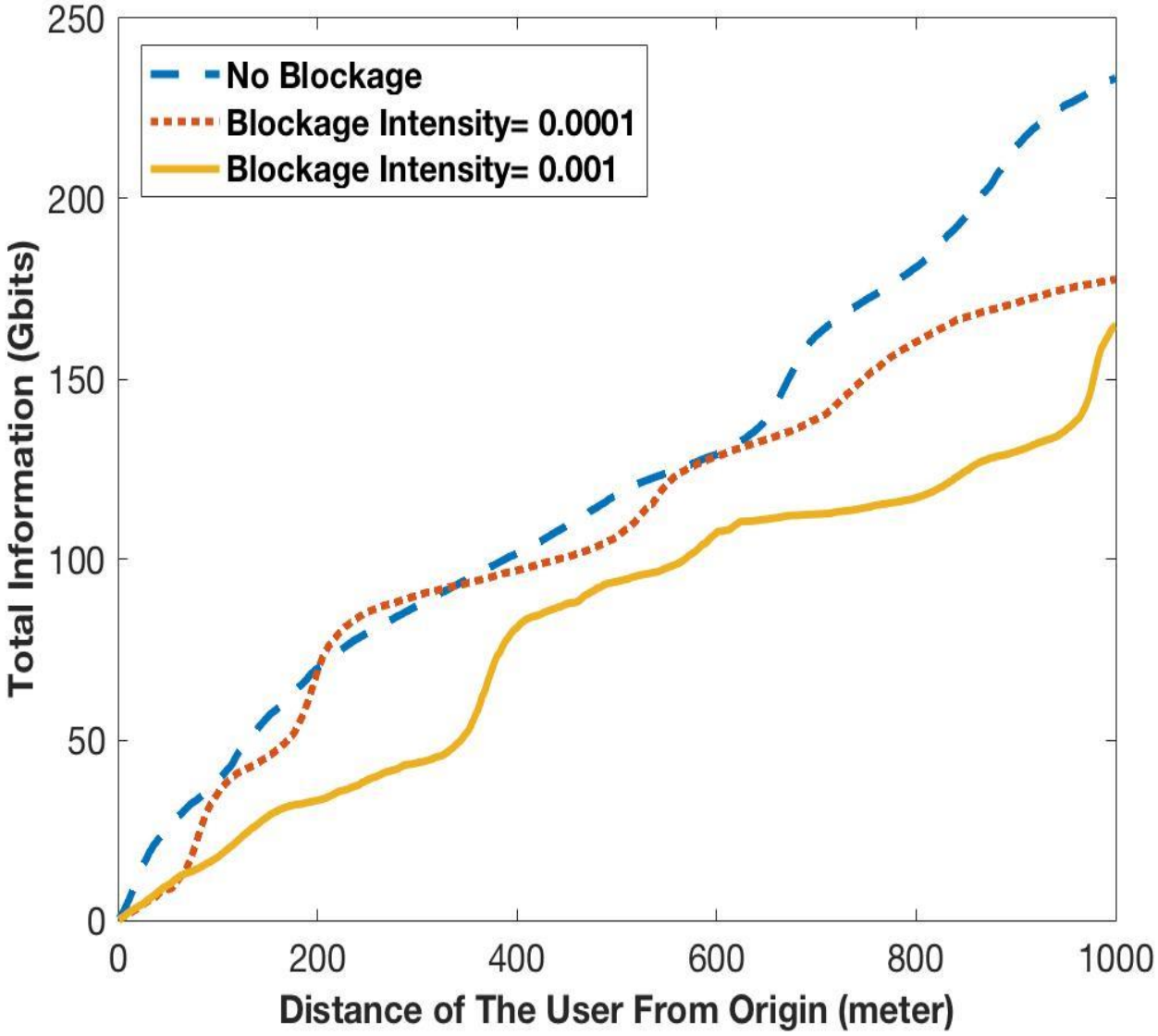

Fig. 2.6. Total information received (Gbits) vs distance (meter) of the user from the origin for cell radius of 200 m for user speed of 1m/s.

$r\ (m)$	$\Lambda = 0$	$\Lambda = 10^{-4}$	$\Lambda = 10^{-3}$
50	0.2001	0.1791	0.1424
100	0.0712	0.0678	0.0310
200	0.0234	0.0178	0.0165

Table 2.2. Average receive information rate (Gbps) for the user speed of 1m/sec for different cell radiuses (r) and blockage intensity (Λ).

$r(m)$	$\Lambda = 0$	$\Lambda = 10^{-4}$	$\Lambda = 10^{-3}$
50	0.2192	0.1857	0.1589
100	0.0911	0.0750	0.0552
200	0.0388	0.0212	0.0180

Table 2.3. Average information rate (Gbps) for different cell radiuses (r) and blockage intensity (Λ) for a user at the origin.

$r(m)$	$\Lambda = 0$	$\Lambda = 10^{-4}$	$\Lambda = 10^{-3}$
50	0	0	0.0150
100	0	0	0.2350
200	0	0	0.5660

Table 2.4. Probability that the user will receive information through a NLOS link (tagged base station in NLOS) for different cell radiuses (r) and blockage intensity (Λ) for a user at the origin.

$r(m)$	$\Lambda = 0$	$\Lambda = 10^{-4}$	$\Lambda = 10^{-3}$
50	0	0.5483	0.9297
100	0	0.4954	0.9699
200	0	0.4725	0.9522

Table 2.5. Probability that a link is NLOS for different cell radiuses (r) and blockage intensity (Λ) for a user at the origin.

$r\ (m)$	$\Lambda = 0$	$\Lambda = 10^{-4}$	$\Lambda = 10^{-3}$
50	40.23	22.58	17.89
100	139.5	66.92	11.12
200	286.5	31.94	13.67

Table 2.6. Average path length for the uninterrupted user association to a base station for different cell radiuses (r) and blockage intensity (Λ).

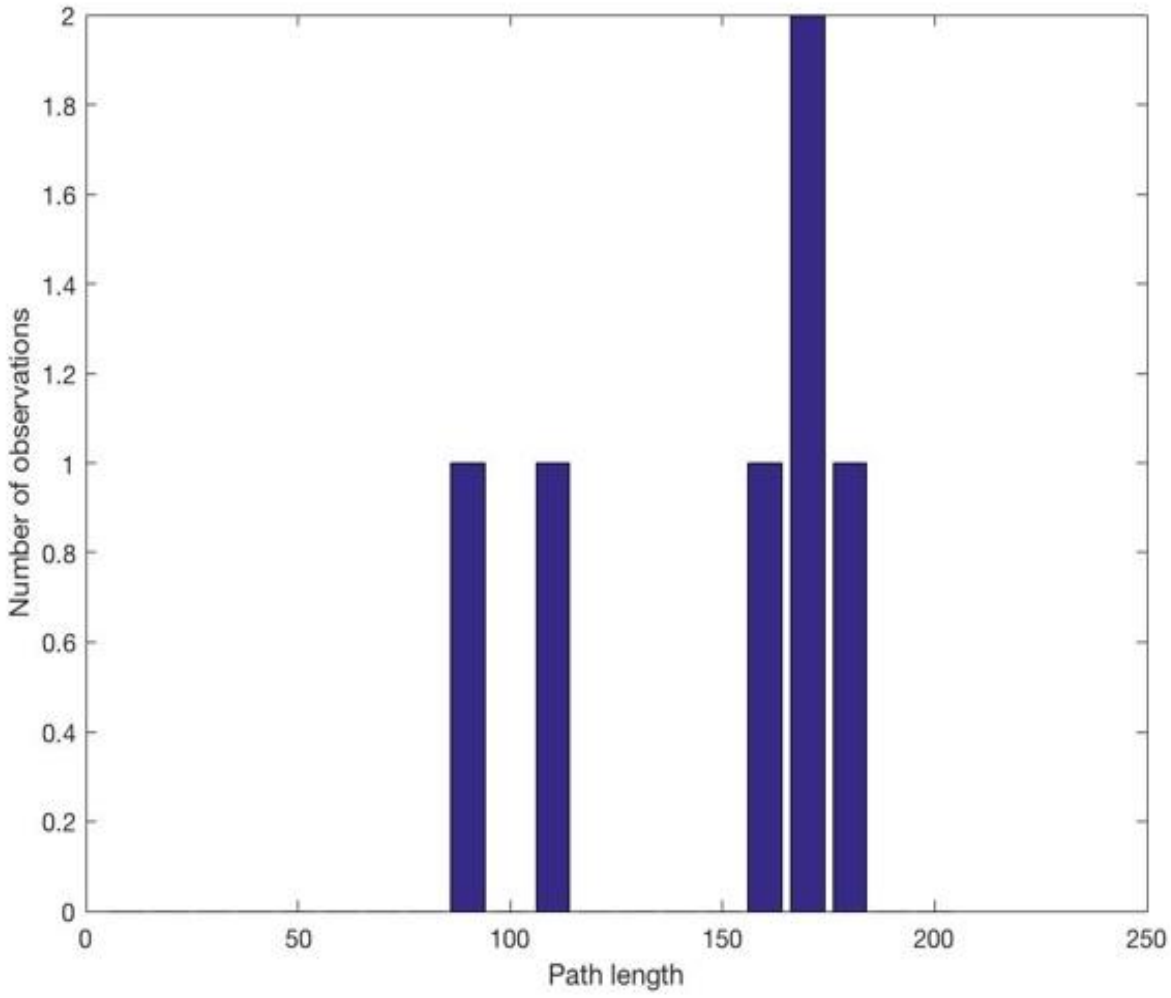

Fig. 2.7. Number of observed uninterrupted path lengths for user association for cell radius of 100m no blocking.

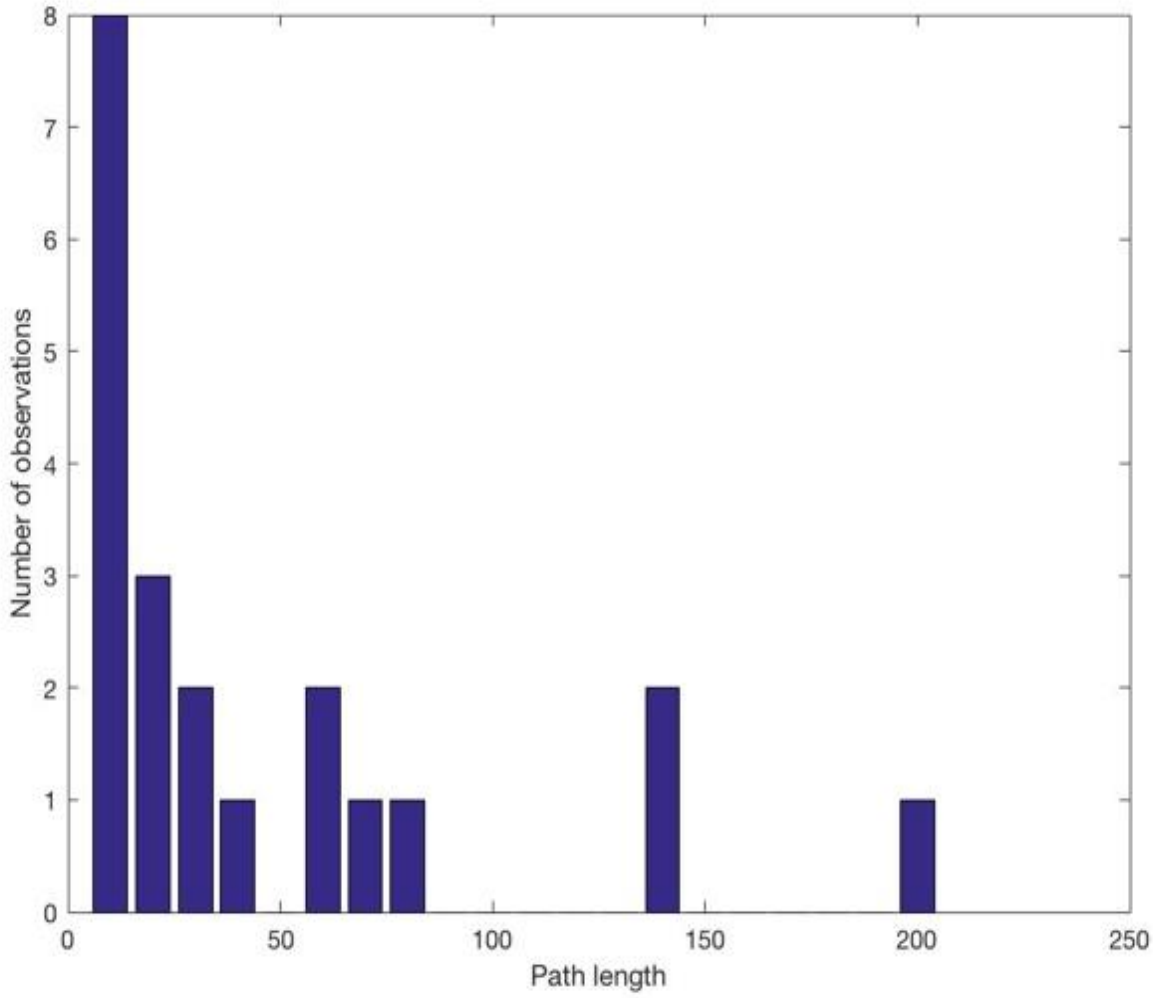

Fig. 2.8. Number of observed uninterrupted path lengths for user association for cell radius of 100m and blocking intensity of 10^{-4}.

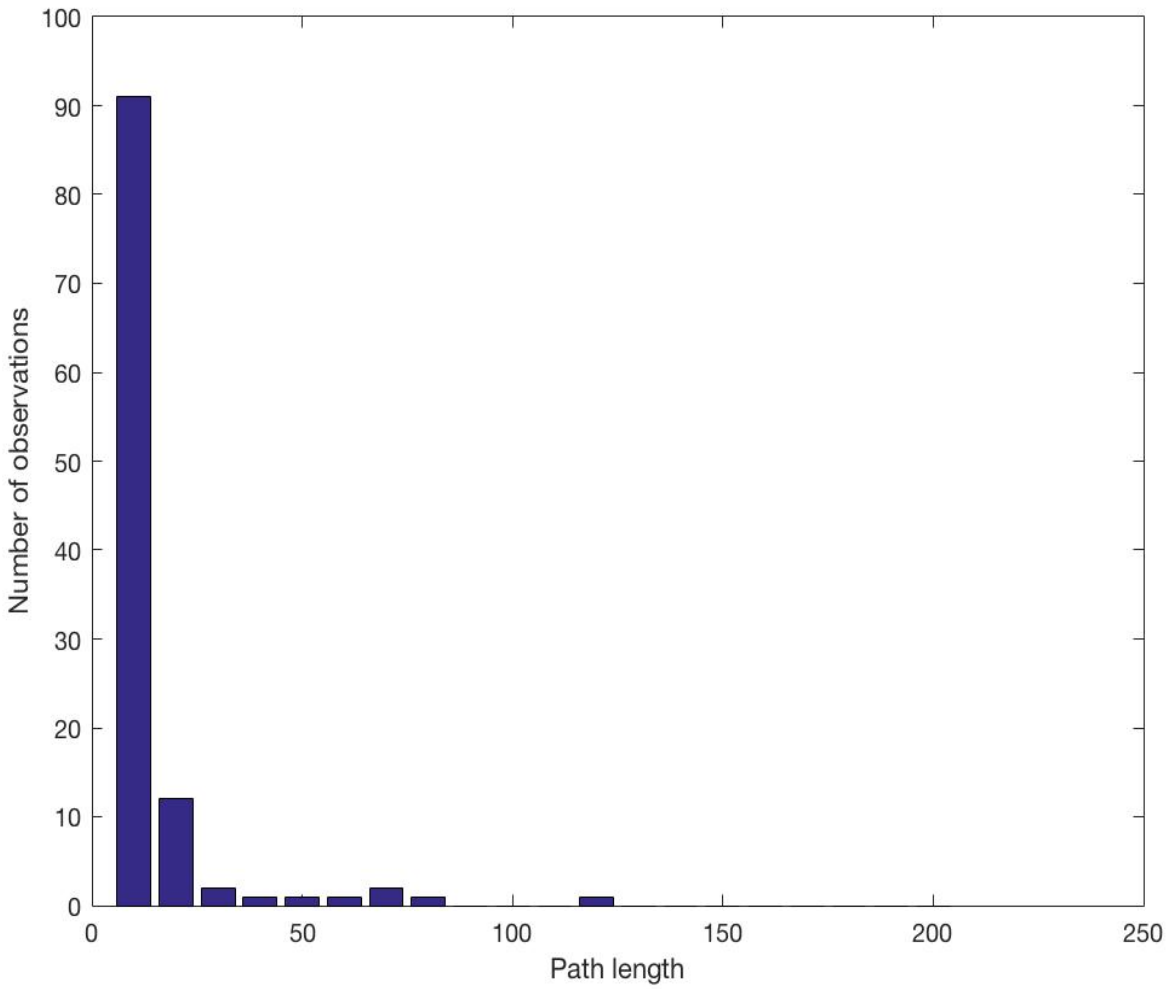

Fig. 2.9. Number of observed uninterrupted path lengths for user association for cell radius of 100m and blocking intensity of 10^{-3}.

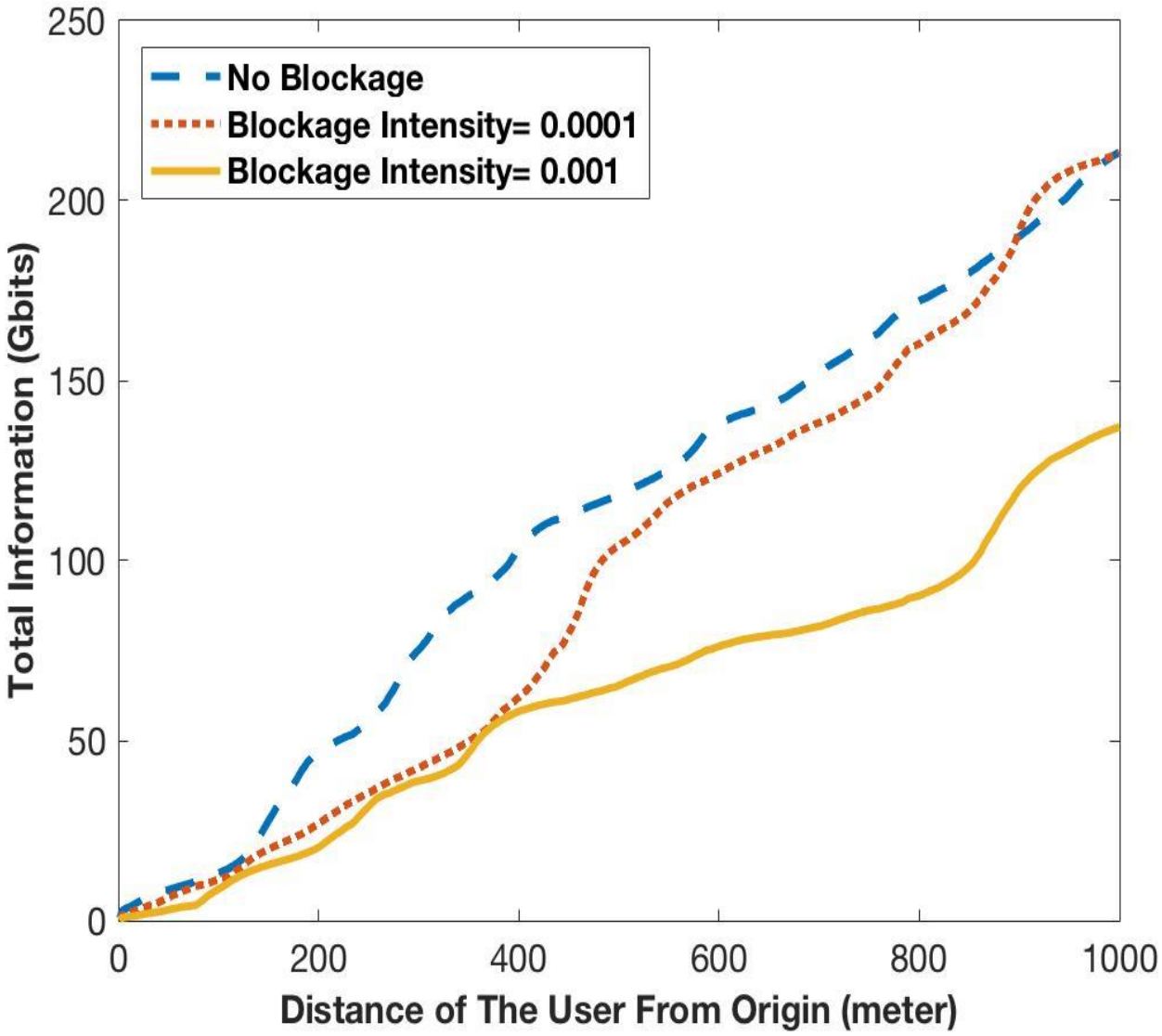

Fig. 2.10. Total information received vs distance of the user from the origin for cell radius of 100 m for user speed in the range [1,6] and mean random interval duration of $\bar{\tau} = 30s$.

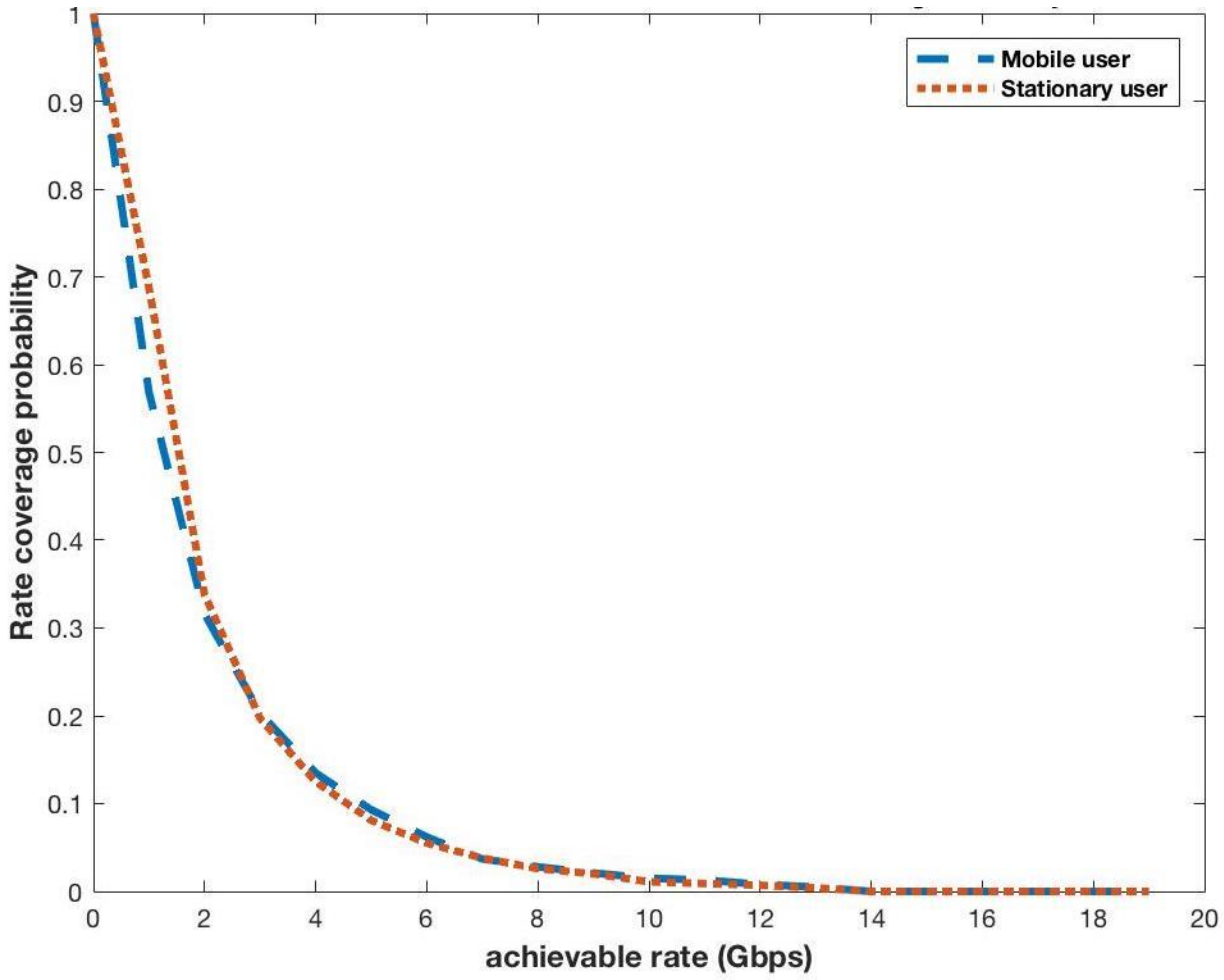

Fig. 2.11. Rate coverage probability vs achievable rate (Gbps) for blockage intensity of 0.001 and cell radius of 50m.

.

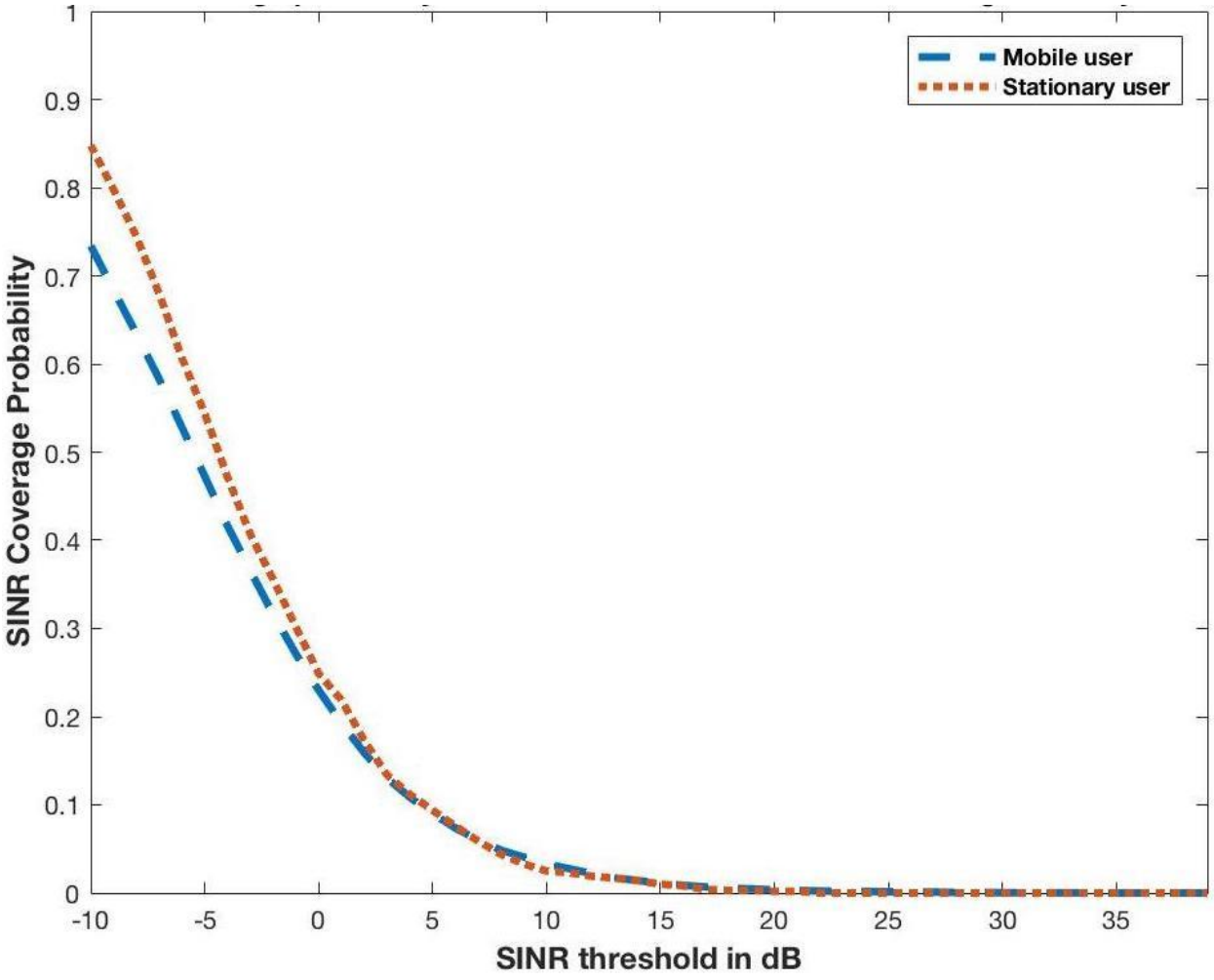

Fig. 2.12. SINR coverage probability vs SINR threshold in dB for blockage intensity of 0.001 and cell radius of 50 meter.

2.5. CONCLUSION

In this chapter, we evaluate performance of a mmWave cellular network with user mobility using Monte Carlo simulation. The results show that the achievable information rate and SINR coverage probability of a mobile user is similar to that of a stationary user. We also determine that average path length that a user is associated with a base station drops down rapidly with the increasing blocking intensity, which will result in high handover rate. Results also show that the increasing user speed results in less cumulative information received by the user as it spends less time traveling the same distance.

CHAPTER 3

DERIVATION OF PROBABILITY DISTRIBUTION OF PATH LENGTH FOR USER ASSOCIATION WITH A BASE STATION

3.1. INTRODUCTION

In this chapter, the probability distribution of path length for no handover is derived as the user moves along a straight line. Handover process is used to provide smooth and continuous network coverage while the mobile user is moving. In handover process the mobile user is transferred from one cell to the neighboring cell with the strongest received power while in active mode. The user will not even be aware of the transfer [12]. MmWave frequencies are very hostile to any type of interruption in the network. The number of handovers can reduce the performance of the network as it increases the control overhead and switching load in to the network [12].

In our work, we determine the uninterrupted path length of the user being associated with the same tagged base station while the user is moving. We derive the theoretical expression for probability of handovers between BSs, as the user is moving. For simplicity we are not considering any blockages in the network topology.

In this chapter –

- First we have determined an analytical expression for the probability of no handover occurring as the user is moving along a straight line. There are three different cases according to the position of the tagged base station.
- Second, we compare the analytical findings with the simulation result. Where we compare the average uninterrupted path length for handover when the cell radius is 50 meters and no blocking on the network. And we also compare the probability of no handover for each segment of path length. from 1 to 1000 meters, where each segment size is 1 meter.

3.2. SYSTEM MODEL

In the following analysis, the probability distribution of no handover will be determined as the user moves along a straight line in small fixed steps of size *d*. In this analysis, we will assume the user moves at a constant speed. We let A_i denote user location at the end of *i*'th step $i = 1,2, \ldots$ with initial user location being A_1. We will let XY denote the line segment between the points *X* and *Y* and the length of this line segment as $|XY|$.

3.2.1. DETERMINING THE PROBABILITY OF NO HANDOVER FOR DIFFERENT LOCATIONS OF TAGGED BASE STATION

Let us consider movement of the user from point A_1 to A_2 as shown in Fig. 3.1. Let *C* denote the tagged based station when the user is at location A_1 and r_1 the distance of *C* from A_1, then $r_1 = |A_1C|$. This means that there is no any base station located within a circle centered at A_1 with radius of r_1. Let r_2 denote the distance of the user when it is located at A_2 from the tagged base station *C*, $r_2 = |A_2C|$. The user to remain associated with the tagged base station *C* when it has moved from A_1 to A_2, then there should not be any station located in a circle centered at A_2 with radius of r_2. We already know that there are no any base stations within the overlap area of those two circles. Thus the user will remain associated with the tagged station *C* at A_2 if there are no base stations located within the non-overlapping area of the circle A_2. Then there are three cases to be considered depending on the location of the tagged base station *C* on the circle centered at A_1. Let θ_1, θ_2 denote the angle between lines A_1C, A_2C and the horizontal axis respectively.

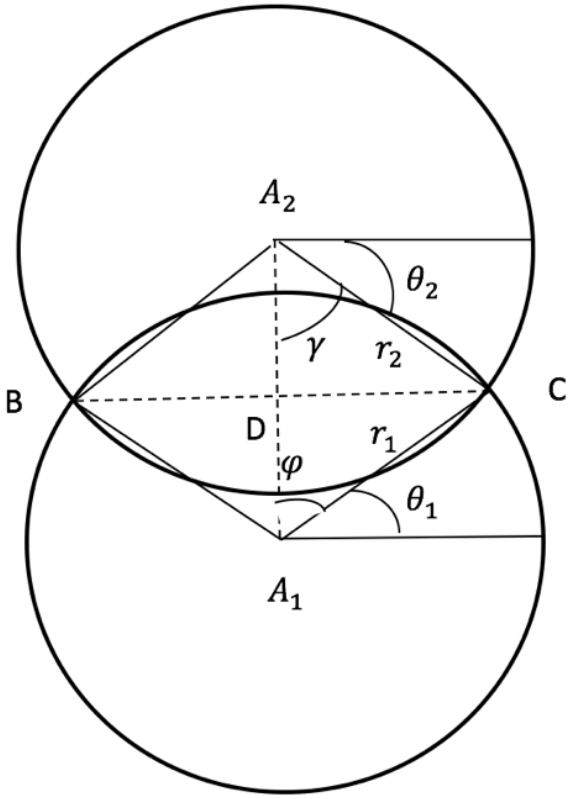

Fig. 3.1. The network diagram when $r_1 sin\theta_1 < d$ and $\theta_1 \leq \frac{\pi}{2}$

Next, we will determine non-overlapping area of the two circles for each of these cases. Since the user moves at steps of size *d*, then $d = |A_1A_2|$. In Fig. 3.1, we let *D* denote the intersection of the lines A_1A_2 and *BC*. Then $|A_1D|$ is given by

$$|A_1D| = r_1 sin\theta_1.$$

Case (i) : when $r_1 sin\theta_1 < d$ and $\theta_1 \leq \frac{\pi}{2}$

From Fig. 3.1, we have the followings,

$$|A_2D| = d - r_1 sin\theta_1,\ |CD| = |BD| = r_1 cos\theta_1 \tag{3.1}$$

$$r_2 = \sqrt{|A_2D|^2 + |CD|^2}$$

Substituting in the above from (3.1),

$$r_2 = \sqrt{(d - r_1 sin\theta_1)^2 + {r_1}^2 cos^2\theta_1} \tag{3.2}$$

In Fig. 3.1, we let γ denote the angle between A_1A_2 and A_2C. Then from the right triangle A_2DC

$$\gamma = cos^{-1}\frac{|A_2D|}{r_2} = cos^{-1}\frac{d - r_1 sin\theta_1}{r_2} \tag{3.3}$$

where the second equation above follows from the substitution from (3.1). Next θ_2 is given by,

$$\theta_2 = \frac{\pi}{2} - \gamma = \frac{\pi}{2} - cos^{-1}\frac{d - r_1 sin\theta_1}{r_2} \tag{3.4}$$

In Fig. 3.1, defining φ as the angle between the lines A_1A_2 and A_1C, then

$$\varphi = \frac{\pi}{2} - \theta_1 \tag{3.5}$$

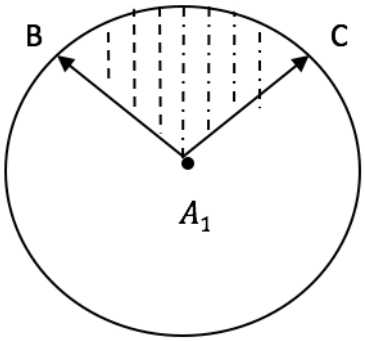

Fig. 3.2. $\widetilde{A_1BC}$ is the smaller of the circular sector of the circle centered at A_1

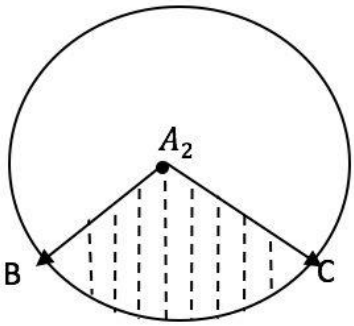

Fig. 3.3. $\widetilde{A_2BC}$ is the smaller of the circular sector of the circle centered at A_2

As shown in Fig. 3.2, let us define $\widetilde{A_1BC}$ as the smaller of the circular sector of the circle centered at $A_1$and the arc $\widetilde{BC}$.

Similarly defining $\widetilde{A_2BC}$ as the smaller of the circular sector of the circle centered at A_2 and the arc $\widetilde{BC}$ in Fig. 3.3. Next, let $S_{\widetilde{A_1BC}}$, $S_{\widetilde{A_2BC}}$ denote the areas of the circular sectors $\widetilde{A_1BC}$, $\widetilde{A_2BC}$ respectively, then,

$$S_{\widetilde{A_2BC}} = \gamma {r_2}^2 = {r_2}^2 cos^{-1} \frac{d - r_1 sin\theta_1}{r_2} \tag{3.6}$$

where the second equation in the above follows from the substitution from (3.3).

$$S_{\widetilde{A_1BC}} = \varphi {r_1}^2 = {r_1}^2 \left(\frac{\pi}{2} - \theta_1\right) \tag{3.7}$$

and in the above second equation follows from (3.5).

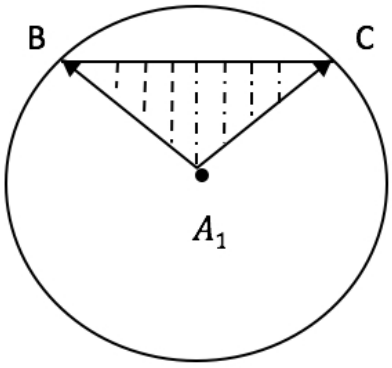

Fig. 3.5. Triangle $\Delta A_1 BC$

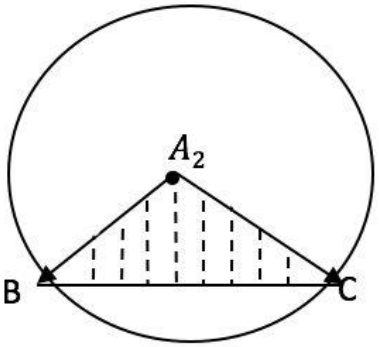

Fig. 3.6. Triangle $\Delta A_2 BC$

Next let $S_{\Delta A_2 BC}$, $S_{\Delta A_1 BC}$ denote the areas of the triangles $\Delta A_2 BC$ and $\Delta A_1 BC$ as shown in Fig.s 3.5 and 3.6 respectively. Then,

$$S_{\Delta A_2 BC} = |A_2 D| * |CD| = (d - r_1 sin\theta_1) r_1 cos\theta_1 \tag{3.8}$$

where the second equation follows from substitution from (3.1).

$$S_{\Delta A_1 BC} = |A_1 D| * |CD| = (r_1 sin\theta_1)\,(r_1 cos\theta_1) = \frac{1}{2} {r_1}^2 sin2\theta_1 \tag{3.9}$$

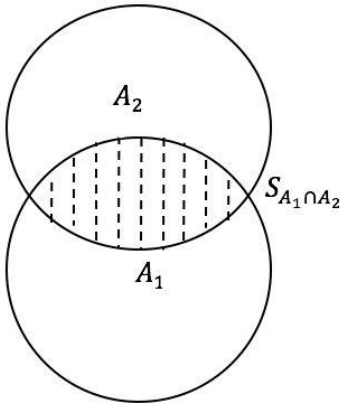

Fig. 3.7. Area of the intersection of the circles centered at $A_1$and A_2

Next let $S_{A_1 \cap A_2}$denote the area of the intersection of the circles centered at $A_1$and A_2 respectively as shown in Fig. 3.7, then,

$$S_{A_1 \cap A_2} = S_{\widehat{A_2BC}} - S_{\Delta A_2BC} + S_{\widehat{A_1BC}} - S_{\Delta A_1BC} \tag{3.10}$$

Substituting in the above from (3.6-3.9), then,

$$S_{A_1 \cap A_2} = {r_2}^2 cos^{-1} \frac{d - r_1 sin\theta_1}{r_2} - (d - r_1 sin\theta_1) r_1 cos\theta_1 + {r_2}^2 \left(\frac{\pi}{2} - \theta_1\right) - \frac{1}{2}{r_1}^2 sin2\theta_1 \tag{3.11}$$

Next, let $S_{A_2 - (A_1 \cap A_2)}$ denote the area of the circle at A_2 that donot overlap with circle A_1 and S_{A_2}area of the circle A_2, then,

$$S_{A_2 - (A_1 \cap A_2)} = S_{A_2} - S_{A_1 \cap A_2} \tag{3.12}$$

where S_{A_2} is given by,

$$S_{A_2} = \pi r_2^2 \tag{3.13}$$

Now, we are ready to determine probability of no hand over as the user moves from point $A_1$to $A_2$for this case,

$$P_r(no\ handover\ |r_1\ and\ \theta_1) = P_r\big(no\ base\ station\ in\ S_{A_2-(A_1\cap A_2)}|r_1\ and\ \theta_1\big) \tag{3.14}$$

Since base stations are located according to a Poisson process with intensity of λ

$$P_r(no\ handover\ |r_1\ and\ \theta_1) = \exp(-\lambda S_{A_2-(A_1\cap A_2)}) \tag{3.15}$$

Substituting in the above from (3.11-3.13) gives,

$$P_r(no\ handover\ |r_1\ and\ \theta_1) = \exp[-\lambda\{\pi {r_2}^2 - [{r_2}^2 cos^{-1}\frac{d-r_1 sin\theta_1}{r_2} - (d - r_1 sin\theta_1)r_1 cos\theta_1 + {r_2}^2\left(\frac{\pi}{2}-\theta_1\right) - \frac{1}{2}{r_1}^2 sin2\theta_1]\}] \tag{316}$$

Case (ii) : when $r_1 sin\theta_1 > d$ and $\theta_1 \leq \frac{\pi}{2}$

This case shown in Fig. 3.8 the derivation of probability of no handover is similar to the previous case.

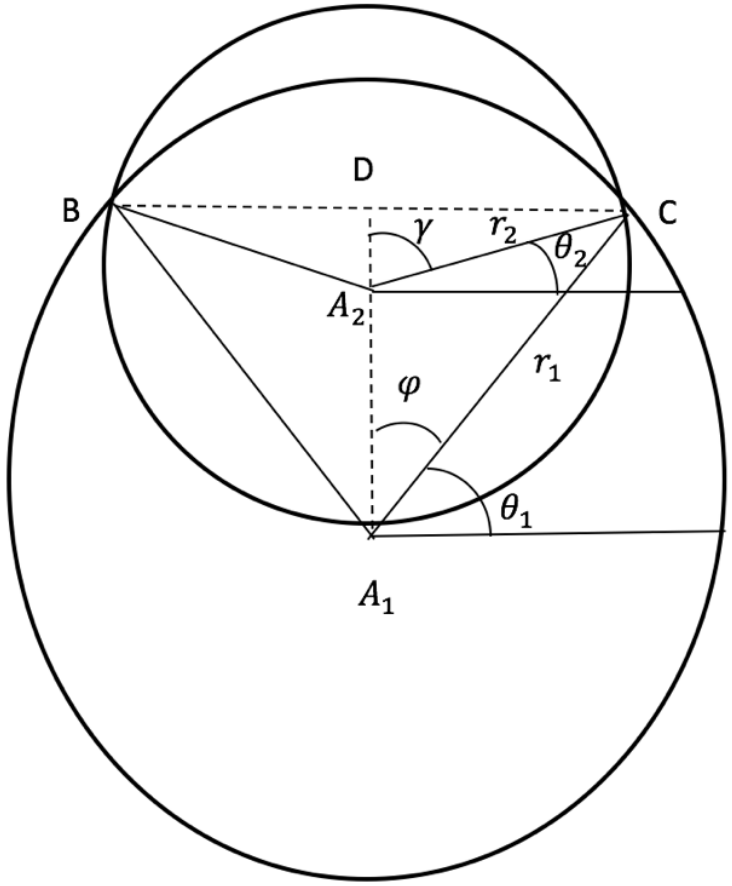

Fig. 3.8. The network diagram when $r_1 sin\theta_1 > d$ and $\theta_1 \leq \frac{\pi}{2}$

From Fig. 3.8, we have the followings, , we let *D* denote the extension of the line A_1A_2 that intersect with *BC*. Then $|A_1D|$ is given by $|A_1D| = r_1 sin\theta_1$.

$$|A_2D| = r_1 sin\theta_1 - d, \quad |CD| = |BD| = r_1 cos\theta_1 \tag{3.17}$$

$$r_2 = \sqrt{|A_2D|^2 + |CD|^2}$$

Substituting in the above from (3.17),

$$r_2 = \sqrt{(r_1 sin\theta_1 - d)^2 + {r_1}^2 cos^2\theta_1} \tag{3.18}$$

In Fig. 3.2, we let γ denote the angle between A_1D and A_2C. Then from the right triangle A_2DC

$$\gamma = cos^{-1}\frac{|A_2D|}{r_2} = cos^{-1}\frac{r_1 sin\theta_1 - d}{r_2} \tag{3.19}$$

where the second equation above follows from the substitution from (3.17).

$$\theta_2 = \frac{\pi}{2} - \gamma = \frac{\pi}{2} - cos^{-1}\frac{r_1 sin\theta_1 - d}{r_2} \tag{3.20}$$

In Fig. 3.2, defining φ as the angle between the lines A_2D and A_1C, then

$$\varphi = \frac{\pi}{2} - \theta_1 \tag{3.21}$$

Let us define $\widetilde{A_1BC}$ as the smaller of the circular sector of the circle centered at A_1 and the arc $\widetilde{BC}$. Similarly defining $\widetilde{A_2BC}$ as the smaller of the circular sector of the circle centered at A_2 and the arc $\widetilde{BC}$. Next let $S_{\widetilde{A_1BC}}$, $S_{\widetilde{A_2BC}}$ denote the areas of the circular sectors $\widetilde{A_1BC}$, $\widetilde{A_2BC}$ respectively, then,

$$S_{\widetilde{A_2BC}} = \gamma {r_2}^2 = {r_2}^2 cos^{-1}\frac{r_1 sin\theta_1 - d}{r_2} \tag{3.22}$$

where the second equation in the above follows from the substitution from (3.19).

$$S_{\widetilde{A_1BC}} = \varphi {r_1}^2 = {r_1}^2\left(\frac{\pi}{2} - \theta_1\right) \tag{3.23}$$

and in the above second equation follows from (3.21).

Next let $S_{\Delta A_2BC}$, $S_{\Delta A_1BC}$ denote the areas of the triangles ΔA_2BC and ΔA_1BC respectively. Then,

$$S_{\Delta A_2BC} = |A_2D| * |CD| = (r_1 sin\theta_1 - d) r_1 cos\theta_1 \tag{3.24}$$

where the second equation follows from substitution from (3.17).

$$S_{\Delta A_1BC} = |A_1D| * |CD| = (r_1 sin\theta_1)\,(r_1 cos\theta_1) = \frac{1}{2}{r_1}^2 sin2\theta_1 \tag{3.25}$$

Next let $S_{A_2-(A_1 \cap A_2)}$ denote the nonoverlapping area of the circles centered at $A_1$and A_2 respectively, then,

$$S_{A_2-(A_1 \cap A_2)} = (S_{\widehat{A_2BC}} - S_{\Delta A_2BC}) - (S_{\widehat{A_1BC}} - S_{\Delta A_1BC}) \quad (3.26)$$

Substituting in the above from (3.22-3.25), then,

$$S_{A_2-(A_1 \cap A_2)} = \left\{ {r_2}^2 cos^{-1} \frac{r_1 sin\theta_1 - d}{r_2} - (r_1 sin\theta_1 - d) r_1 cos\theta_1 \right\} - \{ {r_2}^2 \left(\frac{\pi}{2} - \theta_1 \right) - \frac{1}{2} {r_1}^2 sin2\theta_1 \} \quad (3.27)$$

Now, we are ready to determine probability of no hand over as the user moves from point $A_1$to $A_2$for this case,

$$P_r(no\ handover\ |r_1\ and\ \theta_1) = P_r\left(no\ base\ station\ in\ S_{A_2-(A_1 \cap A_2)} | r_1\ and\ \theta_1\right) \quad (3.28)$$

Since base stations are located according to a Poisson process with intensity of λ,

$$P_r(no\ handover\ |r_1\ and\ \theta_1) = \exp(-\lambda S_{A_2-(A_1 \cap A_2)}) \quad (3.29)$$

Substituting in the above from (3.27) gives,

$$P_r(no\ handover\ |r_1\ and\ \theta_1) = \exp\left\{ -\lambda \left[[{r_2}^2 cos^{-1} \frac{r_1 sin\theta_1 - d}{r_2} - (r_1 sin\theta_1 - d) r_1 cos\theta_1] - [{r_2}^2 \left(\frac{\pi}{2} - \theta_1 \right) - \frac{1}{2} {r_1}^2 sin2\theta_1] \right] \right\} \quad (3.30)$$

Case (iii) : when $\theta_1 \geq \frac{3\pi}{2}$

This case is shown in Fig. 3.9, again derivation of the probability of no handover will be similar to the previous cases. For convenience in this analysis θ_1 will be measured counterclockwise from the horizontal axis.

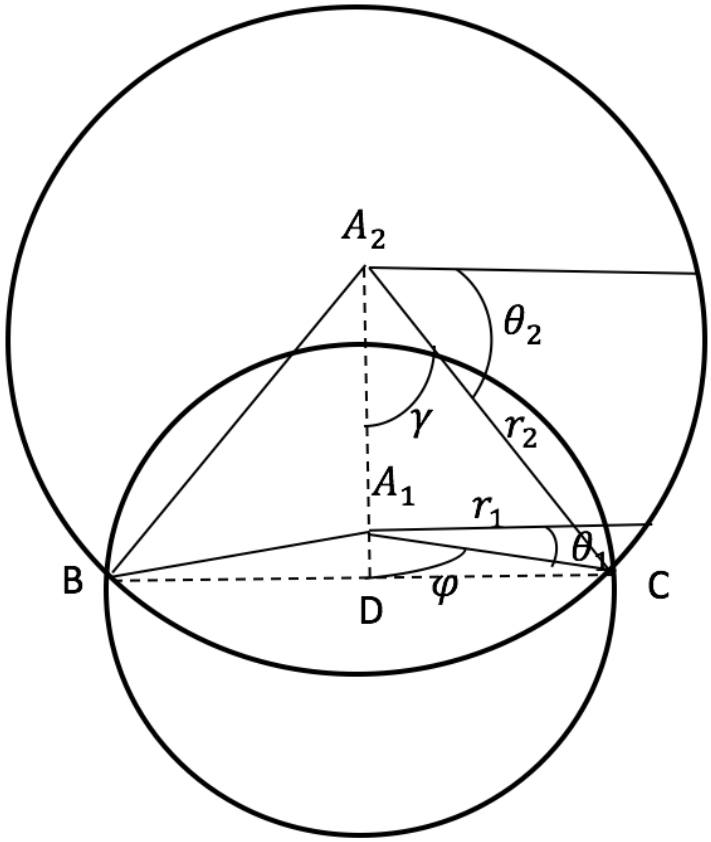

Fig. 3.9. The network diagram when $\theta_1 \geq \frac{3\pi}{2}$

From Fig. 3.9, we have the followings, , we let *D* denote the extension of the line A_1A_2 that intersect with *BC*. Then $|A_1D|$ is given by $|A_1D| = r_1 sin\theta_1$.

$$|A_2D| = r_1 sin\theta_1 + d, \quad |CD| = |BD| = r_1 cos\theta_1 \tag{3.31}$$

$$r_2 = \sqrt{|A_2D|^2 + |CD|^2}$$

Substituting in the above from (3.31),

$$r_2 = \sqrt{(r_1 sin\theta_1 + d)^2 + {r_1}^2 cos^2\theta_1} \tag{3.32}$$

In Fig. 3.9, we let γ denote the angle between A_2D and A_2C. Then from the right triangle A_2DC

$$\gamma = cos^{-1}\frac{|A_2D|}{r_2} = cos^{-1}\frac{r_1 sin\theta_1 + d}{r_2} \tag{3.33}$$

where the second equation above follows from the substitution from (3.31).

$$\theta_2 = \frac{\pi}{2} - \gamma = \frac{\pi}{2} - cos^{-1}\frac{r_1 sin\theta_1 + d}{r_2} \tag{3.34}$$

In Fig. 3.3, defining φ as the angle between the lines A_1D and A_1C, then

$$\varphi = \frac{\pi}{2} - \theta_1 \tag{3.35}$$

Let us define $\widetilde{A_1BC}$ as the smaller of the circular sector of the circle centered at A_1 and the arc $\widetilde{BC}$. Similarly defining $\widetilde{A_2BC}$ as the smaller of the circular sector of the circle centered at A_2 and the arc $\widetilde{BC}$. Next let $S_{\widetilde{A_1BC}}$, $S_{\widetilde{A_2BC}}$ denote the areas of the circular sectors $\widetilde{A_1BC}$, $\widetilde{A_2BC}$ respectively, then,

$$S_{\widetilde{A_2BC}} = \gamma {r_2}^2 = {r_2}^2 cos^{-1}\frac{r_1 sin\theta_1 + d}{r_2} \tag{3.36}$$

where the second equation in the above follows from the substitution from (3.33).

$$S_{\widetilde{A_1BC}} = \varphi {r_1}^2 = {r_1}^2\left(\frac{\pi}{2} - \theta_1\right) \tag{3.37}$$

and in the above second equation follows from (3.35).

Next, let $S_{\Delta A_2BC}$, $S_{\Delta A_1BC}$ denote the areas of the triangles ΔA_2BC and ΔA_1BC respectively. Then,

$$S_{\Delta A_2BC} = |A_2D| * |CD| = (r_1 sin\theta_1 + d) r_1 cos\theta_1 \tag{3.38}$$

where the second equation follows from substitution from (3.31).

$$S_{\Delta A_1 BC} = |A_1 D| * |CD| = (r_1 sin\theta_1)(r_1 cos\theta_1) = \frac{1}{2} {r_1}^2 sin2\theta_1 \quad (3.39)$$

Next let $S_{A_1 \cap A_2}$ denote the area of the intersection of the circles centered at A_1 and A_2 respectively, then,

$$S_{A_1 \cap A_2} = S_{A_1} - [(S_{\widetilde{A_2 BC}} - S_{\Delta A_2 BC}) - (S_{\widetilde{A_1 BC}} - S_{\Delta A_1 BC})] \quad (3.40)$$

where S_{A_1} is given by,

$$S_{A_1} = \pi r_1^2 \quad (3.41)$$

Substituting in the above from (3.36 -3.39) and 3.41, then,

$$S_{A_1 \cap A_2} = \pi r_1^2 - [\{{r_2}^2 \left(\frac{\pi}{2} - \theta_1\right) - \frac{1}{2} {r_1}^2 sin2\theta_1\} - \{{r_2}^2 cos^{-1} \frac{r_1 sin\theta_1 + d}{r_2} -$$

$$(r_1 sin\theta_1 + d) r_1 cos\theta_1\}] \quad (3.42)$$

Next, let $S_{A_2 - (A_1 \cap A_2)}$ denote the area of the circle at A_2 that donot overlap with circle A_1 and S_{A_2} area of the circle A_2, then,

$$S_{A_2 - (A_1 \cap A_2)} = S_{A_2} - S_{A_1 \cap A_2} \quad (3.43)$$

where S_{A_2} is given by,

$$S_{A_2} = \pi r_2^2 \quad (3.44)$$

Now, we are ready to determine probability of no hand over as the user moves from point A_1 to A_2 for this case,

$$P_r(no\ handover\ |r_1\ and\ \theta_1) = P_r\left(no\ base\ station\ in\ S_{A_2 - (A_1 \cap A_2)} | r_1\ and\ \theta_1\right) \quad (3.45)$$

Since base stations are located according to a Poisson process with intensity of λ,

$$P_r(no\ handover\ |r_1\ and\ \theta_1) = \exp(-\lambda S_{A_2 - (A_1 \cap A_2)}) \quad (3.46)$$

Substituting in the above from (3.43 - 3.45) gives,

$$P_r(no\ handover\ |r_1\ and\ \theta_1) = \exp[-\lambda\left\{\pi {r_2}^2 - [\pi r_1^2 - [\{{r_2}^2\left(\frac{\pi}{2} - \theta_1\right) - \right.$$

$$\left.\frac{1}{2}{r_1}^2 sin2\theta_1\} - \{{r_2}^2 cos^{-1}\frac{r_1 sin\theta_1 + d}{r_2} - (r_1 sin\theta_1 + d)r_1 cos\theta_1\}]]\right\}] \quad (3.47)$$

3.2.2. DETERMINING PROBABILITY DISTRIBUTION OF PATH LENGTH WITHOUT HANDOVER

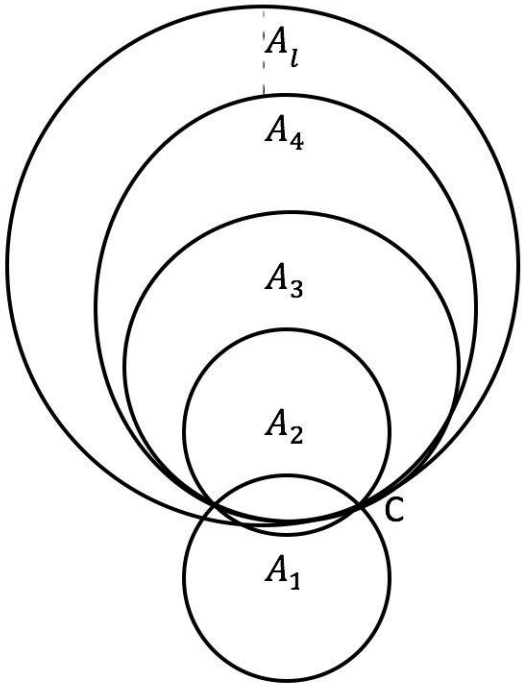

Fig. 3.10. The network diagram for number of cells with one closest base station

First of all, we will consider probability of hand over as the user moves from A_2 to A_3 given that there was no hand over during the movement from A_1 to A_2 and the tagged base station is *C*. This can be done by setting in the derivation of previous subsection,

$$r_1 = r_2 \quad , \qquad \theta_1 = \theta_2 \tag{3.48}$$

and determining new r_2 and θ_2 values from equations (3.2) and (3.4) respectively. Then probability of no hand over may be determined from equations (3.16, 3.30 and 3.47) as the user moves from A_2 to A_3 given that there was no handover during the movement from $A_1$to A_2.

The above procedure may be applied to determine the probability of no handover recursively as the user moves from location A_{i-1} to A_i with $i = 2,3,$ .... given that in the preceding movements steps there was no handover. This scenario is shown in Fig. 3.10, where *C* is the tagged base station.

Next, we will determine probability distribution of path length for no handover. Let us defining,

$$F_\ell = \text{Prob(no handover is at least } \ell \text{ steps)}$$

$$P_\ell = \text{Prob(no handover is } \ell \text{ steps)}$$

Next, let us determine the following conditional probabilities,

define,

$$F_{\ell|r_1,\theta_1} = \text{Prob(no handover is at least } \ell \text{ steps} \mid r_1, \theta_1)$$

$$P_{\ell|r_1,\theta_1} = \text{Prob(no handover is } \ell \text{ steps} \mid r_1, \theta_1)$$

Then, we have,

$$F_{\ell|r_1,\theta_1} = \prod_{i=2}^{\ell+1} \Pr(no\ stations\ in\ S_{A_i-(A_i \cap A_{i-1})} \mid r_1 and\ \theta_1), \ell \geq 1 \tag{3.49}$$

We note that S_{A_i} refers to the area of a circle centered A_i and with radius of A_iC.

$$P_{\ell|r_1,\theta_1} = F_{\ell|r_1,\theta_1} - F_{\ell+1|r_1,\theta_1} \tag{3.50}$$

Finally, unconditional distribution of probability that path length with no hand over equals to ℓ steps is given by,

$$P_\ell = \int_0^{2\pi} \int_0^{\infty} P_{\ell|r_1,\theta_1} f(r_1,\theta_1) dr_1 d\theta_1 \tag{3.51}$$

where $f(r_1,\theta_1)$ is the joint probability density function (pdf) of the location of the tagged base station when the user is at location A_1, next we will determine this joint pdf. Let us define the following probability distribution,

$$G(r_1) =$$

$$Prob(\text{distance of the user when it's at } A_1 \text{to the tagged base station is less than } r_1)$$

$$G(r_1) = 1 - e^{-\lambda\pi r_1^2} \tag{3.52}$$

Then, pdf of the user distance when it's at $A_1$to the tagged base station is given by,

$$g(r_1) = \frac{dG(r_1)}{dr_1} = 2\lambda\pi r_1 e^{-\lambda\pi r_1^2} \quad , \quad r_1 > 0.$$

Since the tagged base station is equally likely to be any where on the circle centered at A_1 and radius of r_1, the pdf of θ_1 is given by,

$$h(\theta_1) = \frac{1}{2\pi} \ , \qquad 0 < \theta_1 < 2\pi \tag{3.53}$$

$$f(r_1,\theta_1) = g(r_1)h(\theta_1) \tag{3.54}$$

The average path length without hand over is given by,

$$\bar{L} = \sum_{\ell=1}^{\infty} \ell P_\ell \tag{3.55}$$

3.3. RESULTS

In this section, we compare the results of this analysis with simulation. We use the same simulation parameters as in chapter 2 to generate the following results. The simulation and analytical results have been generated by Matlab programs which are Appendix A.1 and A.2 respectively.

Table 3.1 shows the average path length for the uninterrupted user association to tagged base station for cell radius (r) 50m and no blockage from both the analysis and the simulation. As may be seen, the two results are quite close to each other. Figures 3.11 and 3.12 show the probability of no handover for the uninterrupted path length for user association for cell radius 50m and no blockage from both analysis and simulation respectively. From the results shown in Fig. 3.11, we can say that it is obvious of having higher probability of handover when the user is crossing more distance. So both from analytical result and simulation result it can be said that there is lower possibility to occur a handover when the user is covering lower path length and probability of handover is higher when the path length is higher.

***r* (*m*)**	***Analysis***	***Simulation***
50	37.58	40.18

Table. 3.1: Average path length for the uninterrupted user association to tagged base station for cell radius (r) of 50m and no blockage.

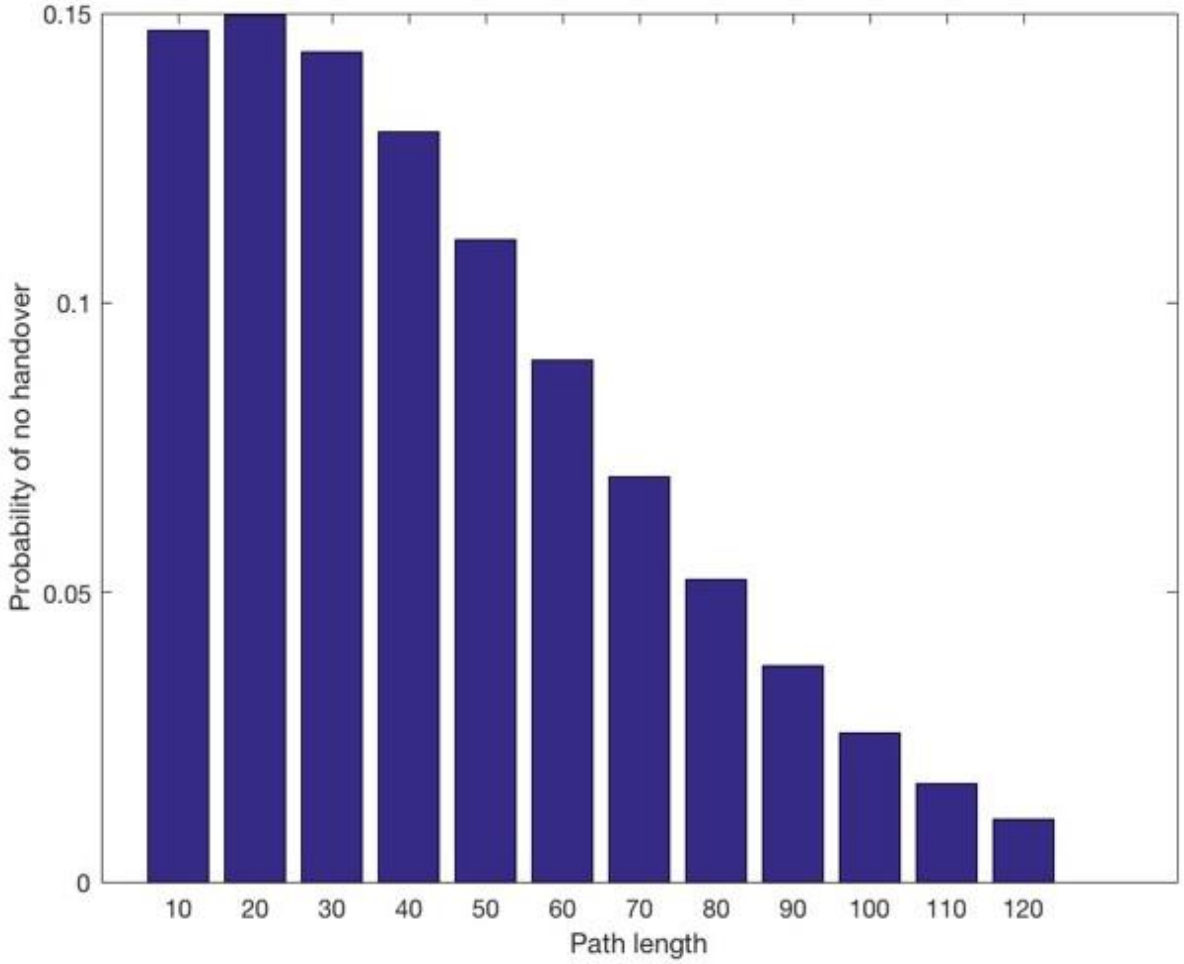

Fig. 3.11. Probability of no handover for uninterrupted path lengths for user association with the same base station for cell radius of 50m and no blocking from the analysis.

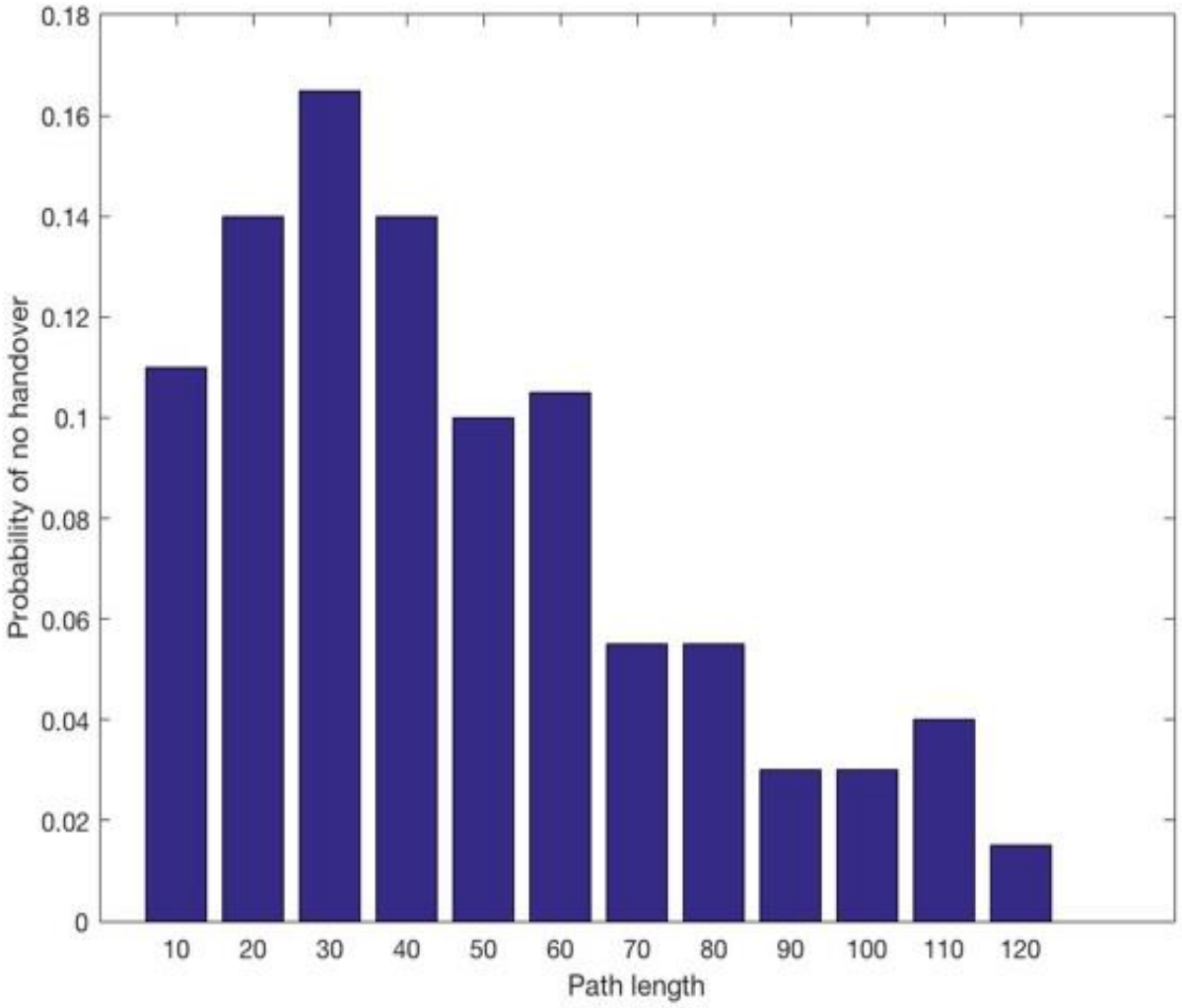

Fig. 3.12. Probability of no handover for uninterrupted path lengths for user association with the same base station for cell radius of 50m and no blocking from simulation.

3.4. CONCLUSION

In this chapter, we have derived probability mass function of uninterrupted path length as the user moves along a straight path assuming no blocking. The analytical and simulation results are in agreement with each other which provides prof that analysis is correct. To the best of our knowledge, this is the first result on the path length distribution of the user with the same base station

CHAPTER 4

CONCLUSION AND FUTURE WORK

4.1. CONCLUSION AND FUTURE WORK

In this thesis, the performance of mmWave cellular networks has been studied which is one of the proposed solutions for the realization of 5G networks. The system performance has been evaluated with user mobility that has not received much research attention. The user is assumed to move along a straight line and the base stations and blockings are located according to independent Poisson Point Processes. The thesis consists of two parts. In the first part, the results have been determined through Monte Carlo simulation and in the second part through analysis. In the first part, we have determined that the average information rate decreases with increasing cell radius and blocking intensity. The cumulative information received by the user is shown to decrease with increasing user speed because travel time decreases. The results show that the rate coverage probability and SINR coverage probability for the mobile user are almost the same as the results for the stationary user. Thus mobility doesnot appear to affect these performance measures. We have also determined uninterrupted path length for the association of the user with the same base station. The results show that uninterrupted path length drops sharply with increasing blocking intensity.

In the second part of the thesis, the impact of the user mobility on the hand over process has been studied analytically. As the user moves its distance to the base stations vary as well the status of their links to the user as LOS and NLOS change. As a result, the base station that user is associated changes as the user moves, which require handovers. The probability distribution of the path length that the user is associated with the same base station has been derived analytically under the assumption that the base stations are distributed according to a PPP process and no blocking. The analytical results show good

agreement with the simulation results. As far as, we know this is the first analytical result on the probability distribution of the path length for the continuous association of a user to a base station. As future work, we propose the extension of this analysis to the case that allows blocking which proved to be challenging.

APPENDIX

MATLAB CODE

A.1. MATLAB CODE FOR SIMULATION RASULTS

```
clc;
clear all;

NRUN = 10;
n_obs = 1000;
cum_average_rate = 0;
SINRT = zeros(n_obs,NRUN);
arrayRate = zeros(n_obs,NRUN);
LLimit = -10;
Limit = -LLimit;
ULimit = 40;
CXProb=zeros(1,Limit+ULimit);
%ULimit=40;
%CXProb=zeros(1,ULimit);
bl_intensity = 0.000;
L=30;
% array=zeros(n_obs,NRUN);
 for xyz=1:NRUN

%********************* initialization of variables ************************

count_y= n_obs;           % declaration the distance along positive Y axis
aL=2;                    % path loss exponent for LOS
aN=4;                    % path loss exponent for NLOS
NagL=3;                  % Nakagami parameter for LOS
NagN=2;                  % Nakagami parameter for NLOS
alphaL=61.4;             % floating intercept for LOS
alphaN=72;               % floating intercept for NLOS
b=2*L*(bl_intensity)/pi;               % beta (depended on blockage density)
%b = 1/141.4;
n=1;                     % declaration of variable
cell=100;                % radius of a cell for each base station
lamda= 1/(pi*(cell)^2);   % base station density
rx=2000;                  % radius of the area taking into consideration
%  totalX= 0;               % initializing summation of variable X
%  A=pi*(rx)^2;             % total area of the simulation
% D=0;                     % initialization variable to count the number of
LOS base stations
MX=2000;                   % NEW max distance between the user and the base
station
Mt = 10;                  % NEW
mt=0.1;                   % NEW
titat = pi/6;             % NEW
Mr = 10;                  % NEW
mr = 0.1;                 % NEW
titar = pi/6;              % NEW
ct = titat/(2*pi);         % NEW
cr = titar/(2*pi);         % NEW
```

```
BW=2*(10^9);                    % User bandwidth
NFigure = 10;
SNoise= -174+10*log10(BW)+NFigure;
SNoise= 10^(SNoise/10);

RX=2000;                  % width of the area taking into consideration
RY=2000;                  % legth of the area under consideration
totalX= 0;                % initializing summation of variable X
A=RX*RY;                  % total area of the simulation

% Generating the blockings

b_poisson=poissrnd(bl_intensity*A);
% The array to store the end points of line blockings
bl_array=zeros(b_poisson,4);
% Determining the ends of each line blocking
for j=1:b_poisson
    XC= RX*rand(1);
    YC= RY*rand(1);
    b_angle=2*pi*rand(1); % angle of blocking
    b_length=0.5*L*rand(1);   % half of length of line blocking
    x1= b_length*cos(b_angle);
    y1= b_length*sin(b_angle);
    X1= XC+x1;
    Y1= YC+y1;
    X2= XC-x1;
    Y2= YC-y1;
    bl_array(j,1)= X1;
    bl_array(j,2)= Y1;
    bl_array(j,3)= X2;
    bl_array(j,4)= Y2;
end



%
%******************** initialization of arrays ****************************


arrayX1 = [];           % array for X axis of all the base stations
arrayY1 = [];           % array for X axis of all the base stations
theta =[];    % NEW
p_segment=zeros(1,count_y); % stores probability of having each segment.
f_segment=zeros(1,count_y);
sum_interefence=zeros(1,count_y);
tag_link=zeros(1,count_y);
%SR=zeros(1,count_y);
Received_power=zeros(1,count_y);
bar_segment=zeros(1,20);
achievable_rate=zeros(1,20);
average_rate = [];
% SINRT=zeros(1,count_y); % SINRT stores the SINR value at each run

% LLimit=1;
% ULimit=40;
```

```
CProb=zeros(1,Limit+ULimit);



D=0;        % D gives probability that tagged based station link is NLOS.
P_NLOS = 0; % P_NLOS gives probability that a link is a NLOS



%****** counting the number of the base station and locating them ********

%  p = 0;     % NEW  counting the number of the base stations
%
%
%  while ( totalX < A )           %  NEW
%      p= p+1;                % NEW
%      u = rand(1);         % uniformly distributed random variable
%      t = rand(1);         % uniformly distributed random variable
%       tu = 2*pi*t;
% %
%      X = ((-1/(lamda))*log(u));    % evaluating a variable X
%      totalX = totalX + X;       % determining the summation of variables X
%      R = sqrt(totalX/pi);          % determining the distance of the base
station from the origin
%      X1 = R*cos(tu);         % determining the X-axis values of each of the
base stations
%      Y1 = X1*tan(tu);         % determining the Y-axis values of each of
the base stations
%      arrayX1 = [arrayX1, X1];  % storing the values of X- axis into an
array
%      arrayY1 = [arrayY1, Y1];  % storing the values of Y- axis into an
array
%      theta =[theta, tu];        % angle of the base stations
% %
%  end

 n_poisson=poissrnd(lamda*A);
%
 for j=1:n_poisson
     X1=RX*rand(1)-RX/2;
     Y1=RY*rand(1)-RY/2;
     tu=atan(Y1/X1);
     arrayX1 = [arrayX1, X1];  % storing the values of X- axis into an array
     arrayY1 = [arrayY1, Y1];  % storing the values of Y- axis into an array
     theta =[theta, tu];        % angle of the base stations
 end
%************************initialization of matrixes**********************

display(arrayX1);
display(arrayY1);

size_X1=length(arrayX1);        % determining the number of X axis values
taking into consideration
r=zeros(1,size_X1);
```

```
ra=zeros(1,size_X1);
n_vector=zeros(1,size_X1);
count_LOS = zeros(1,size_X1);    % initializing a vector that stores the
values for LOS and NLOS
com_state=zeros(1,count_y);
prcom_state=zeros(1,count_y);
arrayRate=zeros(1,count_y);
carrayRate=zeros(1,count_y);
na=zeros(1,count_y);      %to store the tagged station at each y
NGL=zeros(1,size_X1);
NGN=zeros(1,size_X1);

% Generating gamma random variables to be used in the static case

for j=1:size_X1

    NGL(j)=gamrnd(NagL,1/NagL);
    NGN(j)=gamrnd(NagN,1/NagN);
end

%******* determining the distance of each base station for each points while
the user is moving***********

for k=1:count_y

    for j=1:size_X1
        r(j) = 0;
        ra(j)=0;
        count_LOS(j) = 0;
        n_vector(j) = 0;
    end

    for y=1:size_X1      % loop will run until the number of the considered
base station


    r(y)=sqrt(arrayX1(y)^2 + (k-arrayY1(y))^2);   % stores the distance of
each base station at different values of y

   % The equation of the line connecting the user position to the base
   % station
     slopeb = (arrayY1(y)-k)/arrayX1(y);
     interceptb = arrayY1(y)-slopeb*arrayX1(y);

  % fblock=0 no blocking, fblock=1 blocking
   % Determine whether this station is blocked
      fblock = 0;
      for j=1:b_poisson
          temp1= bl_array(j,2)-bl_array(j,1)*slopeb-interceptb;
          temp2= bl_array(j,4)-bl_array(j,3)*slopeb-interceptb;
          temp=temp1*temp2;
          if(temp < 0) % base station is blocked
   % Determining the equation of line blocking
          slope= (bl_array(j,4)-bl_array(j,2))/(bl_array(j,3)-bl_array(j,1));
          intercept= bl_array(j,4)-slope*bl_array(j,3);
```

```
   % Determining the intersection of line blocking and line connecting user
   % and the base station
          x_int=(interceptb-intercept)/(slope-slopeb);
          y_int=slopeb*x_int+interceptb;
   % Determining the distance of the intersection point to the user
         rtemp=sqrt((y_int-k)^2+x_int^2);
   % Determining whether the intersection point is in between the base
   % station and the user.

               if((r(y)-rtemp)>0)
                   fblock = 1;
                    break;
               end
          end
      end

      if (fblock == 0)  % station is not blocked
          ra(y)=r(y)^-aL;
          count_LOS(y) = aL;  % if LOS then it indicates as '2'
      else    % station is blocked
          ra(y)=r(y)^-aN;
              count_LOS(y) = aN;
      end

    end


   for y=1:size_X1
     if(count_LOS(y)==aL)
         ra(y)=ra(y)*10^(-alphaL/10);
     else
         ra(y)=ra(y)*10^(-alphaN/10);
     end
   end




%****************determining the interference, SINR, Rate*****************
 %  display(r);
 %  display(ra);
 %  display(count_LOS);


    [val,idx]= max(ra);
    na(k)=idx;
    if(k> 1 && (na(k) ~= na(k-1)))
        prcom_state(k)=count_LOS(na(k));
    end
   % g= -log(rand(size_X1,1));   % exponential random variable g as fading


   % r=r.*g;        % interference of all other base station except the
connected one
```

```
    f = rand(size_X1,1);        % NEW
    for j=1:size_X1;            % NEW
        if ( f(j) < (cr*ct))
            f(j)= Mr*Mt;
        else if (f(j) < (cr*ct+cr*(1-ct)))
                f(j)=Mr*mt;
            else if (f(j)< (cr*ct+cr*(1-ct)+(1-cr)*ct))
                    f(j)=Mt*mr;
                else
                    f(j)=mt*mr;
                end
            end
        end
    end
  %  r=r.*f;            % NEW

  % g(i) is the product of gamma random variable for the Nakagami fading
  % and the floating intercept.


    for i=1:size_X1
        if(count_LOS(i) == aL)
          g(i)=gamrnd(NagL,1/NagL); % Dynamic Nagakami
       %    g(i)=NGL(i);   % Static Nagakami
       %      g(i)= g(i)*(10^(-alphaL/10));
        else
            g(i)=gamrnd(NagN,1/NagN);
        %    g(i)=NGN(i);
         %    g(i)= g(i)*(10^(-alphaN/10));
        end
        ra(i)=ra(i)*g(i)*f(i);
    end

% h is the product of the gamma value for the base station that the user is
associated
% and the slope intercept

    if(count_LOS(idx) == aL)
            h =gamrnd(NagL,1/NagL);
        %     h=NGL(idx);
        %     h= h*(10^(-alphaL/10));
    else
            h =gamrnd(NagN,1/NagN);
        %     h = NGN(idx);
         %    h= h*(10^(-alphaN/10));
    end

   % h=exprnd(1);              % fading
    %h=1;
    tag_link(k)=val;
    sum_interference(k)=sum(ra)-ra(idx);
   SINR=(h*Mr*Mt*val)/(SNoise+sum_interference(k));     % determining SINR
   Received_power(k)=h*Mr*Mt*val;
   SINRT(k,xyz)=10*log10(SINR);
```

```
    % SINR=h*Mr*Mt*val/(sum(ra));     % determining SINR
    if(SINR < 100)
    Rate= BW*log(1+ SINR);       % determining information rate
    else
        Rate=BW*log(1+100);
    end

    Rate_bits = Rate/(0.693);   % converting rate from nats/sec to bits/sec

    arrayRate(k) = Rate_bits/10^9;
%     arrayRate(k,xyz) = Rate_bits/10^9;   % storing the rates for each
position of the user


    if(count_LOS(idx) == aL)
        com_state(k)=1;
    else
        com_state(k)=2;
        D=D+1;
    end


    for y=1:size_X1
        if(count_LOS(y)==aN)
            P_NLOS=P_NLOS+1;
        end
    end

end

 end    % end of the loop for xyz


for k=1:count_y
    cum_average_rate = cum_average_rate+arrayRate(k);
    for j=1:k
        carrayRate(k)=carrayRate(k)+arrayRate(j);
    end
end

tagged_station=na(1);
j = 1;
for k=2:count_y
    if(na(k)==tagged_station)
        j=j+1;
    else
        p_segment(j)=p_segment(j)+1;
        tagged_station=na(k);
        j=1;
    end
end

total =0;
for j=1:count_y
```

```
    total=total+p_segment(j);
end

for i=1:count_y
        n=i/10;
        j=round(n);
        if( j < n)
            j=j+1;
        end
        if(j < 20)
            bar_segment(j)=bar_segment(j)+p_segment(i);

        else
            bar_segment(20)=bar_segment(20)+p_segment(i);
        end

end

for i=1:20
    bar_segment(i)=bar_segment(i)/total;
end

sum_total =0;
for j=1:count_y
    sum_total=sum_total+p_segment(j);
    p_segment(j)=p_segment(j)/total;
end




% seg-average corresponds to the average segment length that the user is
% associated with the same tagged station.
seg_average=0;

for j=1:count_y
    seg_average=seg_average+p_segment(j)*j;
end

for j=1:count_y
    for i=1:j
        f_segment(j)=f_segment(j)+p_segment(i);
    end
end

% Calculation of the probabilities of achievable rate

% for j=1:count_y
%   temp=arrayRate(j)/(10^9);
%   temp=round(temp);
%   temp=temp+1;
%   achievable_rate(temp)=achievable_rate(temp)+1;
% end
%
```

```
% for j=1:11
%     achievable_rate(j)=achievable_rate(j)/count_y;
% end
%
% for j=1:11
%     for k=j+1:11
%      achievable_rate(j)=achievable_rate(j)+achievable_rate(k);
%     end
% end

for j=1:count_y
  temp=arrayRate(j)/10^9;
  temp=round(temp);
  temp=temp+1;
  achievable_rate(temp)=achievable_rate(temp)+1;
end

for j=1:20
    achievable_rate(j)=achievable_rate(j)/count_y;
end

for j=1:20
    for k=j+1:20
     achievable_rate(j)=achievable_rate(j)+achievable_rate(k);
    end
end

for xr=1:NRUN
    for j=1:count_y

    if(SINRT(j,xr) >= LLimit)
        if(SINRT(j,xr) < ULimit)
          temp=round(SINRT(j,xr));

         if(temp > SINRT(j,xr))
            temp = temp-1;
          end
          CProb(temp+Limit+1)=CProb(temp+Limit+1)+1;
        else
            CProb(ULimit+Limit)=CProb(ULimit+Limit)+1;
        end
    end
end

for j=1:Limit+ULimit
    CProb(j)=CProb(j)/count_y;
end

for j=1:Limit+ULimit
    for k=j+1:Limit+ULimit
      CProb(j)=CProb(j)+CProb(k);
    end
end
```

```
for j=1:Limit+ULimit
    CXProb(j)=CXProb(j)+CProb(j);
    CProb(j)=0;
end
end   % end of xr loop

for j=1:Limit+ULimit
    CXProb(j)=CXProb(j)/NRUN;
end

% end



cum_average_rate = cum_average_rate/(NRUN*count_y);

% display(tag_link);
%  display(na);
% display(prcom_state);
%  display(com_state);
% display(p_segment);
% display(Received_power);
% display(sum_interference);
%   display(SR);
% display(achievable_rate);

size_X1 = size_X1
total = total
sum_total=sum_total

display(arrayX1);
display(arrayY1);

% D corresponds to the probability that the user will receive information
% through a NLOS link.
D=D/count_y
% Probability that a link is NLOS
P_NLOS=P_NLOS/(size_X1*count_y)

% New performance metric for blocking
   normalized_blocking=D/P_NLOS

% Average path segment that a user associated with a tagged base station.
seg_average=seg_average
SNoise=SNoise

cum_average_rate = cum_average_rate

y=1:(count_y);

figure(1)
plot(y,arrayRate)
ylabel('Information Rate Cy (Gbits/sec)')
xlabel('distance of the user from origin(meter)')
```

```
figure(2)
plot(y,carrayRate) % plotting the information rate vs each point of positive
Y-axis
ylabel('Information Rate Cy');
xlabel('distance of the user from origin(meter)');

figure(3)
plot(y,com_state) % plotting the connected base station is LOS or LNOS
axis([0 count_y 0 3]);
ylabel('Los=1 , Nlos=2');
xlabel('distance of the user from origin(meter)');

figure(4)
 x = 10:10:200;
 bar(x,bar_segment);
 ylabel('Probability');
 xlabel('Path length');

x=0:19;

figure (5)
c = plot(x,achievable_rate,':');
set(c,'LineWidth',3);
ylabel('Rate coverage probability')
xlabel('achievable rate (Gbps)')


figure(6)
x = -10:1:39
plot (x,CXProb)
axis ([min(x) max(x) ylim])
% o = plot(x(1,LLimit:ULimit),CXProb(1,LLimit:ULimit),':');
% axis([LLimit ULimit 0 1])
% set(o,'LineWidth',3)
% ylabel('SINR Coverage Probability')
% xlabel('SINR threshold in dB')

total=total
sum_total=sum_total
```

A.2. MATLAB CODE FOR ANALYTICAL RESULTS

```
% Determining path length distribution. The path length distribution is
% determined through the overlap of multiple cells.

clc;
clear all;
digits(32)

r=zeros(1,2);
tita=zeros(1,2);
M=1200;
N=1200;
K=100;
pr=zeros(1,K);
pr_pathlength=zeros(1,K);
pr_pathlengthfinal=zeros(1,K);
SUM=0;

d=1.0;   % user displacement distance
cell_radius = 50;
lamda = 1/(pi*(cell_radius^2));  % base station intensity

% average distance to the closest base station
av_dis = 0;
for i=1:1000
    av_dis=av_dis+i*(2*pi*lamda*i)*exp(-pi*lamda*i^2);
end

sum1=0;
for i=1:N
    for j=1:M
      sum1=sum1+(1/M)*2*pi*lamda*i*exp(-pi*lamda*i^2);
    end
end

for i=1:N
  for j=1:M
       r(1)=i;
       tita(1)= j*(2*pi)/M;
       for k=1:K
           pr(k)=0;
       end
      for k=1:K

      if ( tita(1) <= (pi/2))
   %    tita(1)= j*(2*pi)/M;
       r(2)= sqrt((d-r(1)*sin(tita(1)))^2+r(1)^2*cos(tita(1))^2);
              if(r(1)*sin(tita(1)) <d)
                temp1=r(2)^2*acos((d-r(1)*sin(tita(1)))/r(2));
                temp2= r(1)^2*(pi/2-tita(1));
                temp3=(d-r(1)*sin(tita(1)))*r(1)*cos(tita(1));
                temp4=r(1)^2*sin(2*tita(1))/2;
                temp=exp(-lamda*(pi*r(2)^2-(temp1+temp2-temp3-temp4)));
                pr(k)=temp;
```

```
                tita(2)= 3*pi/2+acos(d-r(1)*sin(tita(1))/r(2));
            %   if(temp < 0.99)
            %       temp=temp
            %   end
              % temp=temp
             else
               temp1=r(2)^2*acos((r(1)*sin(tita(1))-d)/r(2));
               temp2= r(1)^2*(pi/2-tita(1));
               temp3=(r(1)*sin(tita(1))-d)*r(1)*cos(tita(1));
               temp4=r(1)^2*sin(2*tita(1))/2;
               temp5=temp1-temp3;
               temp6=temp2-temp4;
               temp=exp(-lamda*(temp5-temp6));
               pr(k)=temp;
               tita(2)= pi/2-acos((r(1)*sin(tita(1))-d)/r(2));
          %     if(temp < 0.99)
          %         temp=temp
          %     end
             %  temp=temp
             end
      %  temp=temp*(1/M)*2*pi*lamda*i*exp(-pi*lamda*i^2);
      %  pr(k)=temp;
       end   % The end of if statement for M/4.

       if ( tita(1) > ((3/2)*pi))
         %  tita(1)=2*pi-j*(2*pi)/M;
         %   tita(1)=j*(2*pi)/M;
            r(2)= sqrt((d-r(1)*sin(tita(1)))^2+r(1)^2*cos(tita(1))^2);
            temp1= r(2)^2*acos((d-r(1)*sin(tita(1)))/r(2));
            temp2= r(1)^2*(pi/2-(2*pi-tita(1)));
            temp3=(d-r(1)*sin(tita(1)))*r(1)*cos(tita(1));
            temp4=-r(1)^2*sin(2*(tita(1)))/2;
        %    temp4=r(1)^2*2*sin(tita(1))*cos(tita(1))/2;
            temp=(temp2-temp4)-(temp1-temp3);
            tita(2)=3*pi/2+acos((d-r(1)*sin(tita(1)))/r(2));

            temp=exp(-lamda*(pi*r(2)^2-(pi*r(1)^2-(temp))));
            pr(k)=temp;

        % temp=temp*(1/M)*2*pi*lamda*i*exp(-pi*lamda*i^2);

       end % The end of if statement for 3M/4.
        r(1)=r(2);
        tita(1)=tita(2);

         product = 1;

         for zj=1:k
             product=product*pr(zj);
         end
      %   product=product*(pr(k));

         pr_pathlength(k)=pr_pathlength(k)+product*(1/M)*2*pi*lamda*i*exp(-
pi*lamda*i^2);
```

```
      end % The end of k for loop
 %     product=1;
 %     for k=1:K
 %        product=product*pr(k);
 %     end
 %     SUM=SUM+product*(1/M)*2*pi*lamda*i*exp(-pi*lamda*i^2);
  end  % The end of j for loop
end   % The end of i for loop

for j=1:K
    pr_pathlength(j)=2*pr_pathlength(j);
end

pr_pathlengthfinal(1)=1-pr_pathlength(1);
for k=2:K
    pr_pathlengthfinal(k)=pr_pathlength(k-1)-pr_pathlength(k);
end

SUM=0;
SUM2=0;

for k=1:K
    SUM=SUM+k*pr_pathlengthfinal(k);
    SUM2=SUM2+pr_pathlengthfinal(k);
end


 x=1:K;
 plot(x,pr_pathlengthfinal);
 display(pr_pathlength);
 display(pr_pathlengthfinal);
 av_dis=av_dis
 sum1=sum1
 SUM2=SUM2
 SUM=SUM
```

REFERENCES

[1] J. G. Andrews, S. Buzzi, W. Choi, S. Hanly, A. Lozano, A.C.K. Soong, and J. C. Zhang, "What will 5G be", IEEE Journal on Selected Areas in Communications, Vol. 32, No. 6, pp. 1065-1082, 2014.

[2] T. Bai, A. Alkhateeb, and R. W. Heath, "Coverage and capacity of millimeter-wave cellular networks", IEEE Communications Magazine, pp. 70-77, Sept. 2014.

[3] T. Bai, R. Vaze, and R. W. Heath, "Analysis of blockage effects on urban cellular networks", IEEE Transactions on Wireless Communications, Vol. 13, No.9, pp. 5070-5083, 2014.

[4] T. S. Rappaport, G. R. Maccartney, M. K. Samimi, and S. Sun, "Wideband millimeter-wave propagation measurements and channel models for future wireless communication design", IEEE Transactions on Communications, Vol. 63, No. 9, pp. 3029-3056, 2015.

[5] M. R. Akdeniz, Y. Liu, M. K. Samimi, S. Sun, S. Rangan, T. S. Rappaport, and E. Erkip, "Millimeter wave channel modeling and cellular capacity evaluation", IEEE Journal on Selected Areas in Communications, Vol. 32, No. 6, pp. 1164-1179, 2014.

[6] J. G. Andrews, F. Baccelli, and R. K. Ganti, "A tractable approach to coverage and rate in cellular networks", IEEE Transactions on Communications, Vol. 59, No. 11, pp. 3122-3134, 2011.

[7] T. Bai and R.W. Heath, "Coverage and rate analysis for millimeter-wave cellular networks', IEEE Transactions on Wireless Communications, Vol. 14, No. 2, pp. 1100-1114, 2015.

[8] J. G. Andrews, T. Bai, M. N. Kulkarni, A. Alkhateeb, A. K. Gupta, and R.W. Heath, "Modeling and analyzing millimeter wave cellular systems", IEEE Transactions on Communications, Vol. 65, No.1, pp. 404-430, 2017.

[9] M. D. Renzo, “Stochastic geometry modeling and analysis of multi-tier millimeter wave cellular networks”, IEEE Transactions on Wireless Communications, Vol. 14, No.19, pp. 5038-5057, 2015.

[10] S. Singh, MN. Kulkarni, A. Ghosh, and J. G. Andrews, “Tractable model for rate in self-backhauled millimeter wave cellular networks”, IEEE Journal on Selected Areas in Communications, Vol. 33, No. 10, pp. 2196-2211, 2015.

[11] Sheldon M. Ross, “Simulation”, Academic Press, 3rd edition, 2002.

[12] B. U. Kazi and G. Wainer, “Handover enhancement for LTE- advanced and beyond heterogeneous cellular networks”, 2017 International Symposium on Performance Evaluation of Computer and Telecommunication Systems (SPECTS), pp. 1-8, 2017

[13] W. Bao and B. Liang, “Stochastic geometry analysis of user mobility in heterogeneous wireless networks”, IEEE Journal on Selected Areas in Communications, Vol. 33, No. 10, pp. 2212-2225, 2015.

[14] X. Lin, R. K. Ganti, P. J. Fleming and J. G. Andrews, “Towards understanding the fundamentals of mobility in cellular networks”, IEEE Transactions on Wireless Communications, Vol. 12, No. 4, pp. 1686-1698, 2013.

[15] H. Saadeh, W. Almobaideen, K. E. Sabri, “Internet of things : a review to support loT architecture’s design”, 2017 2nd International Conference on the Applications of Information Technology in Developing Renewable Energy Processes & Systems (IT- DREPS), pp. 1-7, Dec 6-8, 2017.

[16] M. B. Yassein, S. Alijawarneh, A. Al-Sadi, 2017 International Conference on Electrical and Computing Technologies and Applications (ICECTA) , pp. 1-5, 2017.

[17] D. Singh, G. Tripathi and A. J. Jara, “A survey of Internet-of-Things: future vision, architecture, challenges and services ,” 2014 IEEE World Forum on Internet of Things(WF-loT), pp. 287-292, 2014.

[18] W. Ejaz, A. Anpalagan, M. A. Imran, M. Jo, M. Naeem, S. B. Qaisar, W. Wang, “Internet of Things (loT) in 5G wireless communications”, IEEE Journals & Magazines, Vol. 4, pp. 10310-10314, 2016.

[19] M. Benisha, R. T. Prabu, V. T. Bai, “Requirements and challenges of 5G cellular systems”, 2016 2nd International Conference on Advances in Electrical, Electronics, Information, Communication and Bio- Informatics (AEEICB), pp. 251-254, 2016.

[20] Y. Niu, Y. Li , D. Jin, L. S, A.V. Vasilakos, “A survey of millimeter wave communications (mmWave) for 5G : opportunities and challenges”, Wireless Networks, Vol. 21, Issue. 8, pp. 2657-2676, 2015.

[21] C. Mavromoustakis, G. Mastorakis, J. Batalla, “Internet of things (loT) in 5G mobile technologies”, Springer Publishing Company, 1st edition, 2016.

[22] “IERC- European Research Cluster on the Internet of Things”, Internet-of things-research.eu, 2017. [Online]. Available: http://www.internet-of-things-research.eu. Accessed: February 19, 2018

[23] “What is the loT?”, IBM, [Online]. Available: https://www.ibm.com/internet-of-things/learn/what-is-iot/. Accessed: February 19, 2018

[24] 5G vision white paper : DMC R&D Center, Samsung Electronics Co. Ltd.

[25] Narendra K. “Internet of services: the ultimate goal of Internet of Things”, Linked in article, [Onilne]. Available: https://www.linkedin.com/pulse/internet-services-ultimate-goal-things-narendra-k-saini/. Accessed: February 18, 2018